

E. BUSVELLE (Grand-Couronne)
R. KHARAB (Rouen)
A. J. MACIEJEWSKI (Toruń)
J.-M. STRELCYN (Rouen)

NUMERICAL INTEGRATION OF DIFFERENTIAL EQUATIONS IN THE PRESENCE OF FIRST INTEGRALS: OBSERVER METHOD

Abstract. We introduce a simple and powerful procedure—the observer method—in order to obtain a reliable method of numerical integration over an arbitrary long interval of time for systems of ordinary differential equations having first integrals. This aim is achieved by a modification of the original system such that the level manifold of the first integrals becomes a local attractor. We provide a theoretical justification of this procedure. We report many tests and examples dealing with a large spectrum of systems with different dynamical behaviour. The comparison with standard and symplectic methods of integration is also provided.

1. Introduction. Frequently we need to integrate numerically a system of ordinary differential equations (ODE's) having some first integrals or an evolutionary partial differential equation admitting some conservation laws. In what follows we will consider exclusively the ODE case, but undoubtedly, our method can also be applied to the case of partial differential equations.

Many examples of systems of ODE's having first integrals can be found in classical mechanics, where Hamiltonian equations are of this type, always having the Hamiltonian as a first integral. The Newtonian many body problem with at least three bodies is an example of a non-integrable system having many first integrals.

Another class of systems of ODE's that always have first integrals is the class of the so called Euler equations on a Lie algebra ([32], [33], [63],

1991 *Mathematics Subject Classification:* 34A50, 34C35, 58F30, 65L06.

Key words and phrases: ordinary differential equations, numerical integration, integrable systems, non-integrable systems, chaotic behaviour.

[65]–[70]). The prototype of equations of this class is the system of the standard Euler equations of motion of a rigid body with a fixed point in the absence of gravity. When the Lie algebra is \mathbb{R}^{2n} endowed with the standard Lie bracket, we recover the class of usual Hamiltonian systems.

The Euler equations on Lie algebras are particularly interesting, because, as was discovered recently, many systems of ODE's governing the motion of rigid bodies in different circumstances, described already by L. Euler, D. Poisson, G. R. Kirchhoff, V. A. Steklov and others, belong to this class ([65]–[70], [48]). Many physically interesting systems of Euler equations on Lie algebras were recently described and studied by O. I. Bogoyavlensky ([11]–[20]).

When the system of ODE's is not integrable, but admits some first integrals, its numerical study is particularly delicate. Indeed, when studying a non-integrable system of ODE's without any known first integrals, except for standard precaution measures, we do not have any control on numerical errors, especially in chaotic regions. When first integrals exist, one can demand from the numerical integration procedure to preserve, at least, the first integrals.

It can be easily understood that this is really a very difficult problem if one sees the huge amount of literature devoted to it (see for example [6], [7], [10], [28], [29], [36], [38], [51], [57]–[61] and references cited in these works). Large parts of these papers were written by astronomers, because this problem was recognized for the first time when studying the Newtonian many body problem and in particular the Kepler problem.

The recent paper ([44]) proves that even for an integrable system this problem can be extremely delicate.

The main aim of this paper is to introduce a simple numerical procedure, or rather a class of them, called by us the *observer method*, derived from control theory (see for example [39]), which preserves very well the first integrals over arbitrary long integration time. This last property will be rigorously proven, at least for some range of parameters. The idea of this method consists in a perturbation of the original system in such a way that the level surface of the first integrals, where the interesting solution lies, is an attractor for the perturbed system.

After some preliminary numerical tests on the planar Kepler problem and the uncoupled harmonic oscillators the observer method is applied to the numerical study of the following four examples: the elliptic orbits with big eccentricities of the spatial Kepler problem, the Gavrilov–Shil'nikov system ([34]), the so-called non-Manakov case of the Euler equations on the Lie algebra $so(4)$ ([1], [11], [12], [32], [40], [41], [49], [69], [80], [82]), and finally the geodesic flow on a compact orientable surface with constant curvature -1 ([22]).

These examples represent four main different types of dynamical behaviour: stable completely integrable systems, completely integrable unstable systems, systems with large regions of chaotic behaviour presenting the so called “coexistence” (see e.g. [55] and [78]) and Anosov systems ([73]).

It is important to note that the results of numerical computations reported in Sections 4–8 clearly indicate that the use of the observer method increases the reliability of numerical integration of the considered system on the level manifold of the first integrals.

As was noted by M. Balabane, one can drastically simplify the observer method reducing it to the method called by us the *penalty method*. Although the penalty method is, from the computational point of view, substantially simpler than the observer method, its field of applications is limited and more careful numerical investigations indicate that in contrast to the observer method, it does not preserve the first integrals so well as the observer method does. Considering the simplicity of the penalty method, we are astonished by its absence in the literature. We only know of the paper [61], where some vaguely related numerical procedure is described. See also [36].

Let us also note the evident relation between the problem studied in this paper and the problem of physical realization of constraints in classical mechanics (see for example [3]).

The paper is organized as follows: in Section 2 we describe the observer and penalty methods. In this section we also briefly discuss the case of so-called *partial first integrals* known also under the name of *invariant relations* (see for example [54], [45], [79]), which generalize the globally defined first integrals. In Section 3 we relate rigorously the observer method to numerical integration of ODE’s. In Section 4 the preliminary tests on the observer method are provided. In Section 5 we study numerically the spatial Kepler problem, and in Section 6 the Gavrilov–Shil’nikov system. In Section 7 we study the Euler equations on the Lie algebra $so(4)$, and finally in Section 8 the geodesic flow on a surface of constant negative curvature.

In Sections 4–8 we report many comparisons of the observer method with different standard Runge–Kutta methods, extrapolation method, penalty method and different symplectic methods of integration.

2. The observer method. Consider a system of ODE’s written in vector form

$$(2.1) \quad dx/dt = F(x),$$

where $F \in C^1(U, \mathbb{R}^p)$ and U is an open subset of \mathbb{R}^p , together with the initial condition

$$(2.2) \quad x(t_0) = x_0,$$

for some $x_0 \in U$. We will call the problem (2.1)–(2.2) the *problem (P)*.

Suppose that $H_1, \dots, H_q \in C^2(U)$, $1 \leq q < p$, are first integrals of the system (2.1). Set

$$H = \begin{pmatrix} H_1 \\ \vdots \\ H_q \end{pmatrix},$$

$H \in C^2(U, \mathbb{R}^q)$, and denote by D_H the derivative of H , i.e. its Jacobian matrix.

Let $\|\cdot\|$ denote the Euclidean norm. Fix $x_0 \in U$ and set $H_0 = H(x_0)$. Define the level set

$$(2.3) \quad \Gamma = \{x \in U : H(x) = H_0\}.$$

We will suppose that the integrals H_1, \dots, H_q are functionally independent on Γ , i.e. for $x \in \Gamma$, $\text{rank}(D_H(x)) = q$. Under this assumption, Γ is a smooth submanifold of U . In general, Γ has many connected components.

Let us underline that in concrete examples it can be difficult to verify if the integrals H_1, \dots, H_q are functionally independent on a given level set Γ (see for example [4], [5], [74], [75]). Concerning the practical side of the observer method, this verification can be neglected.

To carry through successfully the theoretical considerations of this paper we will suppose Γ compact.

Define the set $\tilde{\Gamma}_\varepsilon$ by

$$(2.4) \quad \tilde{\Gamma}_\varepsilon = \{x \in U : r(x, \Gamma) \stackrel{\text{def}}{=} \|H_0 - H(x)\| \leq \varepsilon\}$$

Now, from the implicit function theorem one easily deduces that for sufficiently small ε , $0 < \varepsilon \leq \varepsilon_0$, the connected component Γ_ε of $\tilde{\Gamma}_\varepsilon$ that contains Γ is also a compact subset of U on which the integrals H_1, \dots, H_q are functionally independent.

The above compactness condition occurs quite frequently, in particular, for the Kepler problem for strictly negative energies and for the Euler equations on $so(n)$, $n \geq 3$.

It can be easily seen that if A is a $q \times p$ matrix, $q \leq p$, then the $q \times q$ symmetric matrix AA^T is invertible if and only if A is of maximal rank, i.e. of rank q , where A^T denotes the transposed matrix of A . Thus for every $\xi \in \Gamma$, $D_H(\xi)D_H^T(\xi)$ is invertible. Note also that if AA^T is invertible, then $A^T(AA^T)^{-1}$ is just the Moore–Penrose generalized inverse of A .

As the submanifold $\Gamma = \{x \in U : H(x) = H_0\}$ is compact, it is well known (see for example [43]) that the solution $x = x(t)$ of the problem (P) is defined for all $t \in \mathbb{R}$. Let us consider such a solution. For every $t \in \mathbb{R}$ one has $H(x(t)) = H(x_0) = H_0$.

Together with the problem (P), consider the following perturbed initial value problem (called *problem (PP)*):

$$(2.5) \quad \begin{aligned} \frac{d\xi}{dt} &= F(\xi) + D_H^T(\xi)[D_H(\xi)D_H^T(\xi)]^{-1}K(\xi)(H_0 - H(\xi)), \\ \xi(t_0) &= \xi_0, \end{aligned}$$

where $\xi_0 \in U$ and $K(\xi)$ is a diagonal matrix given by

$$(2.6) \quad K(\xi) = \begin{pmatrix} \theta_1 & 0 & \cdots & 0 \\ 0 & \theta_2 & & \vdots \\ \vdots & & \ddots & \\ 0 & \dots & 0 & \theta_q \end{pmatrix}$$

where $\theta_1, \dots, \theta_q$ are smooth functions on Γ_ε such that

$$(2.7) \quad \eta = \min_{1 \leq i \leq q} \min_{\xi \in \Gamma_\varepsilon} \theta_i(\xi) > 0.$$

On the submanifold Γ , where $H(\xi) = H_0$, the ODE system (2.5) reduces to the initial system (2.1). Consequently, the orbits of both systems coincide on Γ .

We will now show that Γ is the global attractor of the system (2.5) restricted to Γ_ε with an exponential rate of convergence of orbits towards Γ which is exactly controlled. The main point is contained in the following very simple lemma.

MAIN LEMMA. *Let $\xi_0 \in \Gamma_\varepsilon$. Then the unique solution of the problem (PP) is defined for every $t \geq 0$, and for such t ,*

$$(2.8) \quad r(\xi(t), \Gamma) \leq r(\xi_0, \Gamma)e^{-\eta t}$$

where $r(\xi, \Gamma)$ is defined in (2.4). Consequently, $\lim_{t \rightarrow \infty} H(\xi(t)) = H_0$.

Proof. If $\xi_0 \in \Gamma$, then $r(\xi(t), \Gamma) = 0$ and (2.8) is true. Now, let $\xi_0 \in \Gamma_\varepsilon$ and $\xi_0 \notin \Gamma$. We will prove both parts of the lemma simultaneously. To prove that every solution $\xi = \{\xi(t)\}$ of the problem (PP) is defined for every $t > 0$, because Γ_ε is compact, it is sufficient to prove that for every $T > 0$ such that the solution $\{\xi(t)\}_{0 \leq t \leq T}$ is defined, $\{\xi(t)\}_{0 \leq t \leq T} \subset \Gamma_\varepsilon$ (see Chapter II of [43]). Thus, consider the solution $\{\xi(t)\}_{0 \leq t \leq T}$ and let $\varepsilon_t = H_0 - H(\xi(t))$. Then, taking into account (2.5), as $D_H F$ is equal to zero because H is a first integral of the initial non-perturbed equation (2.1), one can write

$$\begin{aligned} \frac{d}{dt} \|\varepsilon_t\|^2 &= -2\varepsilon_t^T D_H(\xi(t)) \frac{d\xi(t)}{dt} \\ &= -2\varepsilon_t^T [D_H(\xi(t))F(\xi(t)) + K(\xi(t))(H_0 - H(\xi(t)))] \\ &= -2\varepsilon_t^T K(\xi(t))\varepsilon_t \leq -2\eta \|\varepsilon_t\|^2. \end{aligned}$$

Therefore

$$\|\varepsilon_t\|^2 \leq \|\varepsilon_0\|^2 e^{-2\eta t}$$

and thus the inequality (2.8) holds for $0 \leq t \leq T$. Consequently, for such t , it has been shown that $\xi(t) \in \Gamma_\varepsilon$ and this finishes the proof.

Suppose that instead of integrating numerically on Γ the problem (P), we integrate numerically the perturbed problem (PP). Taking into account the Main Lemma we can predict intuitively the behaviour of first integrals thanks to the correction term, and hope that if the computed orbits of the perturbed system leave Γ , then the correction term pushes them toward Γ . Hence we can expect to bound the error of the computed first integrals. In the next section we will establish rigorously the above qualitative feature. The method of control of the integration errors through the use of the problem (PP), with perhaps other matrices $K(\xi)$ than (2.6), is the *observer method*.

In what follows we will use two kinds of matrix $K(\xi)$:

- The first one when $\theta_1, \dots, \theta_q$ are constants. In this case we will say that one applies the *simple observer*.
- The second one when

$$\theta_i = \alpha_i \|D_H^T(\xi)[D_H(\xi)D_H^T(\xi)]^{-1}L(\beta)\|^{-1}, \quad 1 \leq i \leq q,$$

where α_i, β_i are some strictly positive numbers, and $L(\beta)$ is the $q \times q$ diagonal matrix with β_1, \dots, β_q on the diagonal. In this case the obtained method will be called the *normalized observer*.

As will be seen in Section 5 when studying the spatial Kepler problem, the simple observer fails for elliptic orbits with big eccentricities, while the normalized observer works very well.

Concerning practical computations with the simple observer method, notice that for its application it is enough to solve a system of q linear equations for one calculation of right hand side of the equation (2.5). In fact, define

$$P(\xi) = D_H^T(\xi)[D_H(\xi)D_H^T(\xi)]^{-1}K(\xi)(H_0 - H(\xi)),$$

the observer perturbation term (see (2.5)). It can be written equivalently as

$$P(\xi) = D_H^T(\xi)y(\xi),$$

where $y(\xi)$ is the unique solution of

$$D_H(\xi)D_H^T(\xi)y(\xi) = K(\xi)(H_0 - H(\xi)).$$

Let us pause now on the nature of the perturbation term in (2.5). For $x_0 \in \Gamma_\varepsilon$, denote by $\Gamma(x_0)$ the manifold $\{\xi \in \Gamma_\varepsilon : H(\xi) = H(x_0)\}$. For $\xi \in \Gamma(x_0)$, all vectors orthogonal to $\Gamma(x_0)$ at ξ are of the form $D_H^T(\xi)y$, where $y \in \mathbb{R}^q$. Thus, the perturbation term in (2.5) is orthogonal to the level manifolds $\Gamma(x_0)$. On the other hand, it is clear that only such perturbations

can be used to improve the reliability of numerical integration on Γ of the system (2.1) using the observer approach.

Now, consider the class of perturbations of the form

$$(2.9) \quad D_H^T(\xi)Y(\xi)(H_0 - H(\xi)),$$

where Y is a $q \times q$ matrix function defined on Γ_ε . It is easy to see that the estimate (2.8) can be obtained along the lines of the proof of the Main Lemma precisely in the case when

$$Y(\xi) = [D_H(\xi)D_H^T(\xi)]^{-1}K(\xi),$$

where $K(\xi)$ is an invertible, not necessarily diagonal, positive definite $q \times q$ matrix depending on $\xi \in \Gamma_\varepsilon$ and satisfying, for some $\eta > 0$,

$$\inf_{\xi \in \Gamma_\varepsilon} y^T K(\xi)y \geq \eta \|y\|^2 \quad \text{for every } y \in \mathbb{R}^q.$$

Finally, consider the case when all functions under considerations are real-analytic. In this case it is easy to see that every $x_0 \in \Gamma$ (see (2.3)) has a neighbourhood $V \subset \mathbb{R}^p$ such that for every vector-valued function $\Phi : V \rightarrow \mathbb{R}^p$ vanishing on Γ one has

$$\Phi(\xi) = Y(\xi)(H_0 - H(\xi)),$$

where $\xi \in V$ and Y is a real-analytic $p \times q$ matrix function defined on V . Thus, at least, in the real-analytic case the form (2.9) of the perturbation is unavoidable.

Now let us drastically simplify the problem (PP) by considering the initial value problem

$$(2.10) \quad \begin{cases} d\xi/dt = F(\xi) + D_H^T(\xi)K(\xi)(H_0 - H(\xi)), \\ \xi(0) = \xi_0. \end{cases}$$

At first glance, the qualitative features of the orbits of (2.10) are similar to those for the problem (PP).

Now, in the same way as in the case of the Main Lemma, one can prove for this initial value problem that for all $t \geq 0$ for which the solution $\xi(t)$ is defined one has

$$(2.11) \quad \frac{d}{dt} \|\varepsilon_t\|^2 = -2\varepsilon_t^T D_H(\xi(t))D_H^T(\xi(t))K(\xi(t))\varepsilon_t,$$

where as before $\varepsilon_t = H_0 - H(\xi(t))$. Unfortunately, in full generality, it is not true that the right side of (2.11) is always a strictly negative number. Indeed, the quadratic form $Q(\varepsilon) = \varepsilon^T AK(\xi)\varepsilon$ on \mathbb{R}^q , where A is a symmetric positive definite matrix, is not necessarily positive definite for $q \geq 2$. Consequently, for the initial value problem (2.10) with $q > 1$, one cannot prove the statement of the Main Lemma.

Consider now the particular case when $K(\xi)$ is the identity matrix. The symmetric matrix $D_H(\xi)D_H^T(\xi)$ is strictly positive definite. Denote by $\lambda(\xi)$ its smallest eigenvalue, $\lambda(\xi) > 0$. In this case (2.11) implies that

$$r(\xi(t), \Gamma) \leq r(\xi_0, \Gamma)e^{-\int_0^t \lambda(\xi(s))ds}.$$

From the compactness of Γ_ε , it follows that $\int_0^\infty \lambda(\xi(s))ds = \infty$. Now, one can deduce that the solution of the problem (2.10) is defined for all $t \geq 0$ and that $\xi(t) \in \Gamma_\varepsilon$ for such t . Thus similarity in the qualitative behaviour of the problems (PP) and (2.10) is formally established when $K(\xi)$ is the identity matrix. Clearly, the same remains true when $K(\xi)$ is proportional to a sufficiently small perturbation of the identity matrix. Like the problem (PP), the problem (2.10) can also be used for numerical integration of (P) with controlled errors on first integrals. This is the *penalty method*. Just as for the observer method, we will also talk about the simple penalty method and the normalized penalty method.

To compare the observer and penalty methods, we underline that the latter is numerically simpler. But in the penalty method the control of error on first integrals is not so good as in the observer method. This will be verified on examples in Sections 5 and 6.

Finally, let us discuss briefly the case of partial first integrals. For more details see the forthcoming paper [56].

Many examples of partial first integrals arise in the study of the Euler–Poisson equations of motion of a heavy rigid body with fixed point (see for example [3], [52], [54]). Many other examples can be found for example in [11]–[18], [45] and [79].

Consider the ODE system (2.1). Let $h \in C^1(U)$ be a function which is not constant on any open subset of U and such that its zero level set $\Gamma_0 = \{x \in U : h(x) = 0\}$ is not empty. Then h is a *partial first integral* of the system (2.1) if there exists a function $l \in C(U)$ such that for all $x \in U$ one has

$$D_h(x)F(x) = l(x)h(x).$$

From our differentiability assumptions one easily deduces that the zero level set Γ_0 is an invariant subset of the ODE system (2.1). This means that Γ_0 is foliated by the orbits of (2.1), i.e. if at some instance an orbit of (2.1) crosses Γ_0 then it remains in Γ_0 until its exit from U .

When $l \equiv 0$, we recover the usual notion of first integral.

In many examples much more intricate situations occur when the invariant set is not of codimension one. To describe this, let us introduce the notion of *q-partial first integrals*.

Suppose now that we have q , $1 \leq q < p$, functions H_1, \dots, H_q which are not constant on any open subset of U and such that the zero level set

$\Gamma_0 = \{x \in U : H_i(x) = 0, 1 \leq i \leq q\}$ is not empty. We assume that the functions H_1, \dots, H_q are functionally independent on Γ_0 . Suppose that there exists a $q \times q$ matrix-valued function L defined on U with entries in $C(U)$ such that

$$(2.12) \quad D_H(x)F(x) = L(x)H(x),$$

where $H(x)$ is the column vector (H_1, \dots, H_q) . In this case the vector-valued function H is called a q -partial first integral.

Just as for partial first integrals, also here the zero level set $\Gamma_0 = \{x \in U : H(x) = 0\}$ is an invariant subset for the ODE system (2.1).

Let us underline that in general the functions H_1, \dots, H_q are not necessarily partial first integrals. Examples of such q -partial first integrals can be found, for example, in the problem of the motion of a rigid body with a fixed point (see [52]).

As in the case of first integrals, we suppose that the set Γ_0 is compact.

We would like to have a reliable procedure to integrate numerically the initial value problem (P) on the invariant set Γ_0 . To this end, we define the initial value problem (PPP):

$$(2.13) \quad \begin{aligned} \frac{d\xi}{dt} &= F(\xi) + D_H^T(\xi)[D_H(\xi)D_H^T(\xi)]^{-1}[K(\xi) - L(\xi)]H(\xi), \\ \xi(t_0) &= \xi_0, \end{aligned}$$

where $\xi_0 \in \Gamma_\varepsilon$ which is defined by (2.4) with $H_0 = 0$, and where the $q \times q$ matrix K satisfies (2.6) and (2.7). In the case when H_1, \dots, H_q are first integrals, i.e. when $L(x) \equiv 0$, we recover the problem (PP).

Taking into account (2.12) it is very easy to see that for the problem (PPP), the Main Lemma and its proof remain valid word for word, if only the matrix-valued function L is smooth. Thus also in the case of partial first integrals one can hope to use the perturbed problem (PPP) for reliable integration of the system (2.1) on the invariant manifold Γ_0 .

3. The observer method and numerical integration of ODE's.

As the system (2.5) is autonomous, to integrate numerically the problem (PP) we will use an explicit one-step method

$$(3.1) \quad \xi_{j+1} = \xi_j + h\phi(\xi_j, h)$$

with *increment function* ϕ .

As usual, we will suppose that this method is at least of *order one*, i.e. that for every $\xi_0 \in U$ and $t \geq 0$ such that the solution ξ of the problem (PP) is defined on $[0, t + 1]$, there exists a constant $C(\xi_0, t) > 0$ such that for every $t \geq 0$ and for every $h, 0 < h \leq 1$, one has

$$(3.2) \quad \|\xi(t+h) - \xi(t) - h\phi(\xi(t), h)\| \leq C(\xi_0, t)h.$$

We suppose, of course, the method to be *consistent*, i.e. $\phi(\xi, 0) = \widehat{F}(\xi)$, where \widehat{F} is the right hand side of (2.5) (see [50] for more details).

Now, just as for all standard explicit one-step methods, like the Euler and Runge–Kutta methods, we suppose that for any compact subset $Q \subset U$,

$$(3.3) \quad \sup_{\xi \in Q} \sup_{0 \leq h \leq 1} \|\phi(\xi, h)\| \stackrel{\text{def}}{=} \phi_Q < \infty.$$

Likewise, we suppose that

$$(3.4) \quad \sup_{\xi_0 \in Q} \sup_{0 \leq h \leq 1} |C(\xi_0, h)| \stackrel{\text{def}}{=} C_Q < \infty.$$

When the step $h > 0$ is fixed, instead of the orbits $x(t) \equiv \xi(t)$ with $x(t_0) = \xi(t_0) = \xi_0 \in \Gamma$ of the problem (PP) we compute numerically *the pseudo-orbit* $\{\xi_j\}$. In general, it is a very difficult problem to understand the relation between the true orbits and the related pseudo-orbits (see for example [8], [45]).

The following theorem makes rigorous the main feature of the observer method already indicated in Section 2.

THEOREM 3.1. *Consider the initial value problem (PP). Then for every $\varepsilon > 0$, there exists $h, 0 < h < 1$, small enough and η defined by (2.7) large enough such that if $\xi_0 \in \Gamma$ then $\xi_j \in \Gamma_\varepsilon$ for every $j \geq 0$, i.e.*

$$r(\xi_j, \Gamma) \stackrel{\text{def}}{=} \|H_0 - H(\xi_j)\| \leq \varepsilon$$

where $\{\xi_j\}$ is defined by (3.1).

Proof. First, let us fix the notations and the parameters necessary for the proof.

For $a \in \mathbb{R}^p$, define $d(a, \Gamma) = \inf_{b \in \Gamma} \|a - b\|$. For $r > 0$, set

$$U_r(\Gamma) = \{\xi \in \mathbb{R}^p : d(\xi, \Gamma) \leq r\}.$$

As Γ is compact, $U_r(\Gamma)$ is also compact.

From our assumption on the functional independence of the integrals H_1, \dots, H_q , it follows that for sufficiently small $\varepsilon > 0$, there exist numbers δ_ε and $D_\varepsilon, 0 < \delta_\varepsilon \leq D_\varepsilon$, such that

$$(3.5) \quad U_{\delta_\varepsilon}(\Gamma) \subset \Gamma_\varepsilon \subset U_{D_\varepsilon}(\Gamma) \subset U_{2D_\varepsilon}(\Gamma) \subset U.$$

Define (cf. (3.3) and (3.4))

$$(3.6) \quad \begin{aligned} \phi_\varepsilon &= \phi_{\Gamma_\varepsilon}, & L_\varepsilon &= \sup_{\xi \in U_{2D_\varepsilon}(\Gamma)} \|D_H(\xi)\|, \\ C_\varepsilon &= C_{U_{2D_\varepsilon}(\Gamma)}, & \widehat{F}_\varepsilon &= \sup_{\xi \in \Gamma_\varepsilon} \|\widehat{F}(\xi)\|, \end{aligned}$$

where \widehat{F} is the right hand side of (2.5). Now choose h such that

$$(3.7) \quad 0 < h \leq \min\left(\frac{\delta_\varepsilon}{\phi_\varepsilon}, \frac{\delta_\varepsilon}{\widehat{F}_\varepsilon}, \frac{\varepsilon}{2L_\varepsilon C_\varepsilon}, 1\right).$$

For fixed h , choose η such that $e^{\eta h} > 1$, for example,

$$(3.8) \quad e^{\eta h} \geq 2.$$

This condition is satisfied for $\eta h \geq 0.69$.

Let us return to the pseudo-orbit $\{\xi_j\}_{j \geq 0}$ defined by (3.1). Denote by $\widetilde{\xi}_j$ the value at time h of the solution of the system (2.5) satisfying the initial condition $\xi(0) = \xi_{j-1}$, $j \geq 1$. From the Main Lemma we know that if $\xi_{j-1} \in \Gamma_\varepsilon$ then $\widetilde{\xi}_j$ is well defined and $\widetilde{\xi}_j \in \Gamma_\varepsilon$.

The proof of the theorem is by induction. For $j = 0$ from (3.1) one has

$$\xi_1 - \xi_0 = h\phi(\xi_0, h)$$

and thus from (3.7) one obtains

$$\|\xi_1 - \xi_0\| \leq h\phi_\varepsilon \leq \delta_\varepsilon.$$

As $\xi_0 \in \Gamma$, from (3.5) one deduces then that $\xi_1 \in \Gamma_\varepsilon$.

Now suppose that $\xi_k \in \Gamma_\varepsilon$ for $0 \leq k \leq j$. By (3.1), exactly in the same way as for $j = 0$, we obtain $\|\xi_{j+1} - \xi_j\| \leq \delta_\varepsilon$. On the other hand, from the mean value theorem and (3.7) one has

$$\|\widetilde{\xi}_{j+1} - \xi_j\| \leq h\widehat{F}_\varepsilon \leq \delta_\varepsilon.$$

Thus, $\xi_{j+1}, \widetilde{\xi}_{j+1} \in \overline{B}(\xi_j, \delta_\varepsilon) = \{x \in \mathbb{R}^p : \|x - \xi_j\| \leq \delta_\varepsilon\}$.

Since, by assumption, $\xi_j \in \Gamma_\varepsilon$, from (3.5) we have $\xi_j \in U_{D_\varepsilon(\Gamma)}$ and thus $\overline{B}(\xi_j, \delta_\varepsilon) \subset U_{2D_\varepsilon(\Gamma)} \subset U$. Taking into account the convexity of $\overline{B}(\xi_j, \delta_\varepsilon)$ and (3.6) one has

$$\begin{aligned} r(\xi_{j+1}, \Gamma) &= \|H(\xi_{j+1}) - H_0\| \leq \|H(\widetilde{\xi}_{j+1}) - H_0\| + \|H(\xi_{j+1}) - H(\widetilde{\xi}_{j+1})\| \\ &\leq r(\widetilde{\xi}_{j+1}, \Gamma) + L_\varepsilon \|\xi_{j+1} - \widetilde{\xi}_{j+1}\|. \end{aligned}$$

Now, taking into account the Main Lemma, (3.1) and (3.2) one obtains

$$\begin{aligned} r(\xi_{j+1}, \Gamma) &\leq e^{-\eta h} r(\xi_j, \Gamma) + L_\varepsilon \|\widetilde{\xi}_{j+1} - \xi_j - h\phi(\xi_j, h)\| \\ &\leq e^{-\eta h} r(\xi_j, \Gamma) + L_\varepsilon C_\varepsilon h. \end{aligned}$$

This inequality remains valid with j replaced by k , $0 \leq k \leq j$, because $\xi_k \in \Gamma_\varepsilon$ by our inductive assumption.

Thus for every k , $0 \leq k \leq j$, one has

$$r(\xi_{k+1}, \Gamma) \leq e^{-\eta h} r(\xi_k, \Gamma) + L_\varepsilon C_\varepsilon h.$$

Taking into account this inequality, (3.7) and (3.8) one obtains

$$r(\xi_{j+1}, \Gamma) \leq e^{-\eta h} [e^{-\eta h} r(\xi_{j-1}, \Gamma) + L_\varepsilon C_\varepsilon h] + L_\varepsilon C_\varepsilon h$$

$$\begin{aligned}
&= e^{-2\eta h} r(\xi_{j-1}, \Gamma) + e^{-\eta h} L_\varepsilon C_\varepsilon h + L_\varepsilon C_\varepsilon h \leq \dots \\
&\leq \left(\sum_{s=0}^j e^{-s\eta h} \right) L_\varepsilon C_\varepsilon h < \frac{L_\varepsilon C_\varepsilon h}{1 - e^{-\eta h}} \leq \varepsilon.
\end{aligned}$$

Thus $\xi_{j+1} \in \Gamma_\varepsilon$ and our inductive proof is finished.

Note that as the proof of Theorem 3.1 is based only on the Main Lemma, the theorem remains valid for the problem (PPP) given by (2.13).

Although we considered here only the explicit one-step method, there is no doubt that similar results also hold for multi-step methods, both explicit and implicit.

Note also that the condition (3.8) gives the first restriction on the size of η and thus on the matrix $K(\xi)$. In what follows, when applying the observer method to concrete examples, we will try to choose $\theta_1, \dots, \theta_q$ in such a way as to diminish the possible stiffness ([50]) of the problem (PP) and to improve the quality of the numerical computations.

We will see in the examples below that even if ηh is small, the observer method can work very well.

The explicit exact computations can be given in the case of the simple harmonic oscillator defined by the Hamiltonian

$$H(p, q) = \frac{1}{2}(p^2 + q^2),$$

for the Euler method with the simple observer applied to the first integral H and its value H_0 . These computations prove that for $h > 0$ sufficiently small and $\theta > 0$ such that $2h < \theta$, the limit

$$\lim_{t \rightarrow \infty} H(\xi_t) = R(h, \theta) > H_0$$

exists and that

$$\lim_{h \rightarrow 0} R(h, \theta) = H_0.$$

This means that for such h and θ , the error in H , i.e. $H - H_0$, tends to some small non-zero value.

Finally, note that all preceding considerations can be easily adapted to the case of a compact connected component of a possibly non-compact manifold Γ .

4. The preliminary tests on the observer method. In this section we present two simple examples illuminating main features of the observer method: the planar Kepler problem and the double harmonic oscillator.

The computations were performed on a VAX 4000 computer with double precision of the VAX FORTRAN.

4.1. The planar Kepler problem. It is well known that the Euler method of numerical integration of ODE's gives, in general, very poor results and cannot be used for reliable integration except for a very short time interval. This, in particular, is the case for the planar Kepler problem ([44]). But, as will be seen below, when one uses the Euler method with the simple observer, the results of integration are of good quality over a quite long time interval.

In polar coordinates (r, φ) on the plane, the Hamiltonian H describing the planar Kepler problem is

$$H(r, \varphi, p_r, p_\varphi) = \frac{1}{2} \left(p_r^2 + \frac{p_\varphi^2}{r^2} \right) - \frac{\mu}{r},$$

where μ is a real strictly positive number.

The corresponding Hamilton equations are

$$\begin{cases} \dot{r} = \frac{\partial H}{\partial p_r} = p_r, \\ \dot{\varphi} = \frac{\partial H}{\partial p_\varphi} = \frac{p_\varphi}{r^2} - \frac{\mu}{r^2}, \\ \dot{p}_r = -\frac{\partial H}{\partial r} = \frac{p_\varphi^2}{r^3}, \\ \dot{p}_\varphi = -\frac{\partial H}{\partial \varphi} = 0. \end{cases}$$

Thus, in particular, p_φ is a first integral of the above system.

For a fixed value of p_φ , the first and third equations of this system constitute an independent system of two ODE's, called the reduced system, describing the radial component of the Keplerian motion.

For convenience we will write briefly p instead of p_r . The reduced system

$$(4.1) \quad \begin{cases} \dot{r} = \frac{\partial H_1}{\partial p} = p, \\ \dot{p} = -\frac{\partial H_1}{\partial r} = \frac{p_\varphi^2}{r^3} - \frac{\mu}{r^2} \end{cases}$$

is a Hamiltonian system, with the Hamiltonian function

$$H_1(r, p) = \frac{1}{2} \left(p^2 + \frac{p_\varphi^2}{r^2} \right) - \frac{\mu}{r}.$$

Thus H_1 is a first integral of the reduced system. We will now integrate numerically the elliptic orbit of the reduced system corresponding to $H_1 = -0.4$. We will use three different methods: the adaptive Runge-Kutta-Fehlberg method of order 4(5) with control error 10^{-6} (briefly RKF method),

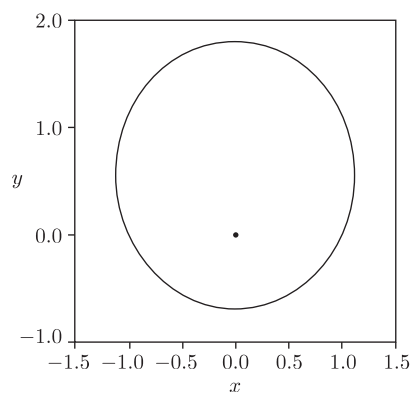


Fig. 1. The reference orbit for the planar Kepler problem in Cartesian (x, y) coordinates.

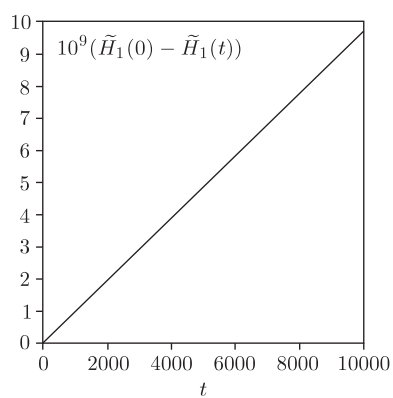


Fig. 2. Errors of the computed reduced Hamiltonian \tilde{H}_1 of the planar Kepler problem integrated numerically by the RKF method.

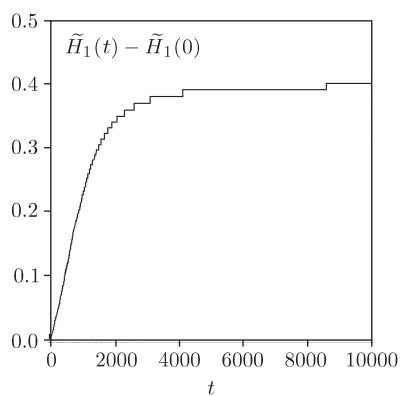


Fig. 3. Errors of the computed reduced Hamiltonian \tilde{H}_1 of the planar Kepler problem integrated numerically by the Euler method.

the Euler method with a fixed step-size $h = 10^{-2}$ and the Euler method as above together with the simple observer method.

Denote by $(\tilde{r}(t_i), \tilde{p}(t_i))_{i \geq 0}$ the computed orbit of the reduced system (4.1). The integration by RKF method gives Figure 1. The error in the computed Hamiltonian $\tilde{H}_1(t_i) = H_1(\tilde{r}(t_i), \tilde{p}(t_i))$ increases linearly with time (see Figure 2), but is smaller than 10^{-8} up to integration time $t = 10000$. This will be the reference trajectory because it can be considered as a very good approximation of the true orbit.

Later on, when considering a first integral, its symbol with a tilde will denote the numerically computed value of this integral.

Applying the Euler method, one can observe that the computed Hamiltonian H_1 increases very quickly, and that after the approximate value of time $t = 6000$, one observes its apparent stabilization (see Figure 3). Moreover, the observed jumps of the computed Hamiltonian correspond, for small

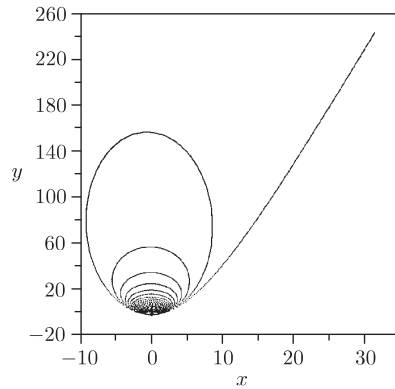


Fig. 4. Destruction of an elliptic orbit computed by the Euler method.

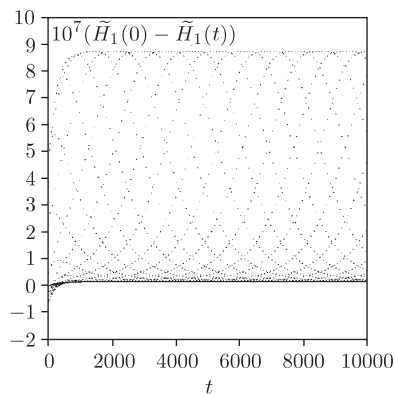


Fig. 5. Errors of the computed reduced Hamiltonian \tilde{H}_1 of the planar Kepler problem for the Euler method with the simple observer method.

time, to the passage through the pericenter—the point of the orbit nearest to the origin.

When time increases, the computed Hamiltonian strongly increases and our initially elliptic orbit becomes hyperbolic as $r \rightarrow \infty$ (see Figure 4).

Thus, the numerical errors inherent in the Euler method destroy completely the phase portrait of the reduced system (4.1) and this occurs for a very short time interval of integration. On the contrary, when one uses the same Euler method as above with the simple observer with $H = H_1$ and $\theta = 1$, one obtains quite good results. After the integration time $t = 10000$, the computed orbit is always elliptic, exactly as in Figure 1, and the error in the computed Hamiltonian is smaller than $5 \cdot 10^{-6}$. In fact, the strong variations of this error are related to the passage through the pericenter of the orbit (see Figure 5). Let us emphasize that, in this example, application of the simple observer improves preservation of the integral 10^6 times.

4.2. The double harmonic oscillator. Our aim is now to study how different applications of the simple observer method improve results when the equations of motion of the double harmonic oscillator are integrated by the Euler method. For this purpose we will study numerically the system of two uncoupled oscillators described by the Hamiltonian

$$(4.2) \quad H_2(q, p) = \frac{1}{2}(p_1^2 + p_2^2 + q_1^2 + q_2^2).$$

It is obvious that $H_1(q, p) = \frac{1}{2}(p_1^2 + q_1^2)$ is also a first integral of the Hamiltonian system defined by the Hamiltonian H_2 .

We chose the initial condition for which $H = (H_1, H_2) = (1.5, 1.9)$. The results of computation by the Euler method with step-size $h = 0.001$ are shown in Figure 6(a). Integration with the same step-size when the simple

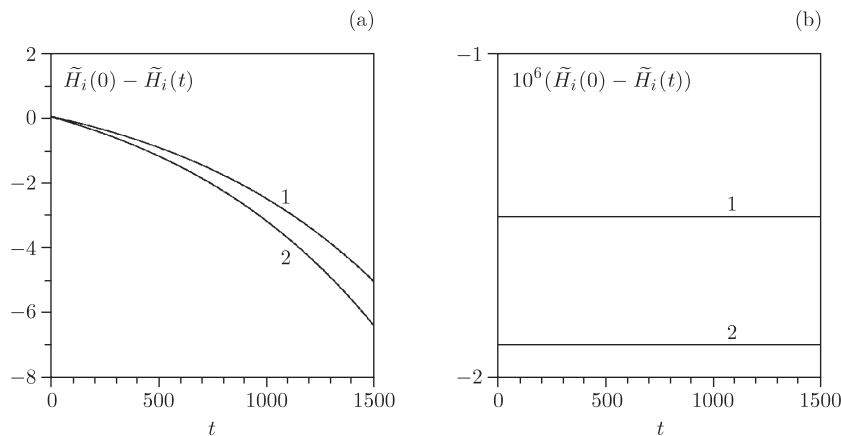


Fig. 6. Errors of the computed first integrals: (1) \tilde{H}_1 and (2) \tilde{H}_2 of the double harmonic oscillator obtained by: (a) the Euler method; (b) the Euler method with the simple observer method applied to both integrals. The step-size was $h = 0.001$.

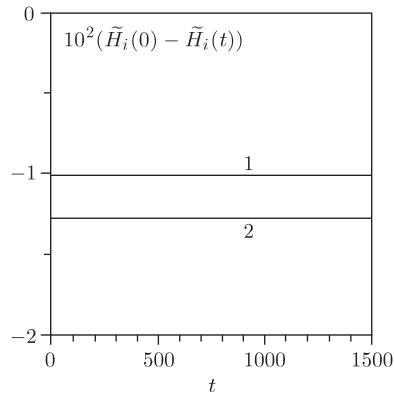


Fig. 7. The same as in Figure 6(b) for step-size $h = 0.1$.

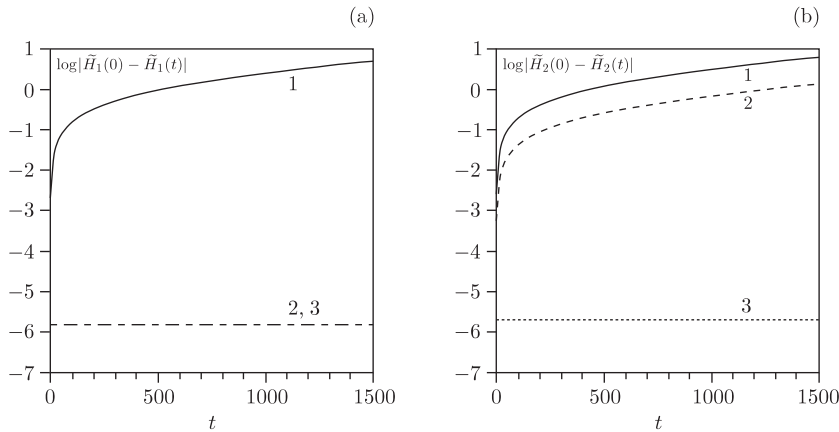


Fig. 8. Errors in the computed first integrals: (a) \tilde{H}_1 , (b) \tilde{H}_2 obtained by: (1) the Euler method, (2) the Euler method with the simple observer method applied to H_1 , (3) the Euler method with the simple observer method applied to H_2 .

observer method is applied for both integrals with $\theta_1 = \theta_2 = 1000$ gives the results reported in Figure 6(b). For the step-size $h = 0.1$ the Euler method is worthless. After 55 steps the absolute values of the errors for both integrals are bigger than 1. For longer time span of integration these errors grow rapidly. However, for the the same step-size when the simple observer method is applied for the two integrals and $\theta_1 = \theta_2 = 15$ we obtain quite satisfactory results (see Figure 7).

Now let us compare the behaviour of the integrals H_1 and H_2 when the Hamiltonian system defined by the Hamiltonian H_2 is integrated by the Euler method as above, and by the Euler method with the simple observer but applied only to: $H = H_1$ on the level manifold $H_1(q, p) = 1.5$, and $H = H_2$ on the level manifold $H_2(q, p) = 1.9$, respectively. To obtain a

reasonable size of error on the first integral H_2 during integration with the Euler method we chose the step-size $h = 10^{-3}$. To satisfy the inequality (3.8) when the simple observer is used, we chose $\theta = 10^3$. The results presented in Figures 8(a) and 8(b) indicate that the use of the observer method improves the preservation of non-observed first integrals. This phenomenon will be confirmed in all our further computations.

5. The spatial Kepler problem

5.1. Description of the system. Consider the classical Kepler problem in \mathbb{R}^3 ([2], [71]). In Cartesian coordinates $(q_1, q_2, q_3, p_1, p_2, p_3)$ of its phase space \mathbb{R}^6 , this problem is described by the Hamiltonian

$$H = \frac{1}{2}(p_1^2 + p_2^2 + p_3^2) - \frac{\mu}{q},$$

where $q = \sqrt{q_1^2 + q_2^2 + q_3^2}$ and μ is a real, strictly positive number.

We will use vectorial notation below, so we put

$$\mathbf{q} = (q_1, q_2, q_3), \quad \mathbf{p} = (p_1, p_2, p_3),$$

and for any vector \mathbf{v} its length will be denoted by v , i.e. $v^2 = \mathbf{v} \cdot \mathbf{v}$, where the dot denotes scalar product.

Besides the Hamiltonian, the Kepler system has other first integrals which are the components of the angular momentum \mathbf{c} and the components of the so-called Laplace vector \mathbf{e} (see [71]). They are defined as follows:

$$(5.1) \quad \mathbf{c} = \mathbf{q} \times \mathbf{p}, \quad \mu \mathbf{e} = \mathbf{p} \times \mathbf{c} - \frac{\mu}{q} \mathbf{q}.$$

The vector \mathbf{c} is perpendicular to the plane of motion. For $c \neq 0$, the vector \mathbf{e} is directed from the origin of the coordinate system to the pericenter. For $c = 0$, the orbits are straight lines passing through the origin, \mathbf{e} is always collinear with the radius vector \mathbf{q} and has length 1. When $c \neq 0$, the length e of the vector \mathbf{e} is equal to the eccentricity of the orbit.

All those seven first integrals of the problem are not functionally independent. In fact, the following relations hold:

$$\mathbf{c} \cdot \mathbf{e} = 0, \quad Hc^2 = \mu^2(e^2 - 1),$$

where H is the value of the Hamiltonian (energy).

In the configuration space $\mathbb{R}^3\{\mathbf{q}\}$, for $c \neq 0$ every orbit lies on a fixed plane passing through the origin and perpendicular to the vector \mathbf{c} . For $H < 0$ and $c \neq 0$ all orbits are periodic. In this case each orbit is an ellipse with focus at the origin, semi-major axis $a = -\mu/(2H)$ and eccentricity e . The orientation of an ellipse in $\mathbb{R}^3\{\mathbf{q}\}$ is traditionally given by means of the Euler angles (Ω, i, ω) . More precisely: Ω —the longitude of the ascending node—is the angle between the first axis of $\mathbb{R}^3\{\mathbf{q}\}$ and the line of

intersection of the orbital plane and the (q_1, q_2) -plane (this line is called the line of nodes), i —the inclination—is the angle between the vector \mathbf{c} and the q_1 -axis, ω —the argument of the pericenter—is the angle between the line of nodes and the vector \mathbf{e} .

The Kepler system appears, among others, in celestial mechanics as the unperturbed problem of more complicated systems describing, e.g., models of planetary systems. Its numerical integration shows generally what kind of problems we can meet integrating planetary equations for long time intervals. The main problem is the accumulation of energy errors because it causes substantial changes of the angular frequency of the periodic motion and therefore stimulates a rapid growth of the errors of position along the orbit which is also perturbed. This is especially true for highly eccentric orbits.

For the Kepler problem we can apply the observer method in many different ways choosing different subsets of integrals. However, it is reasonable to consider only H and \mathbf{c} because, generally, in the many body problem only these integrals are known. It is well known that the level sets $H = \text{const} < 0$ and $c = \text{const} > 0$ are compact.

In our tests we have applied the observer and penalty methods with integrals $H_1 = H$ and $H_2 = c^2$. Write $\mathcal{H} = (H_1, H_2)^T$. Let us verify where these integrals are independent. It is easy to show that

$$(5.2) \quad D\mathcal{H}(\mathbf{q}, \mathbf{p}) = \begin{pmatrix} \frac{\mu}{q^3} \mathbf{q} & \mathbf{p} \\ 2\mathbf{p} \times \mathbf{c} & 2\mathbf{c} \times \mathbf{q} \end{pmatrix}.$$

Evidently, for $c = 0$, i.e. for straight line orbits, the rank of the above matrix is one.

Assume now that $\mathbf{c} \neq \mathbf{0}$. The rank of (5.2) will not be maximal iff

$$(5.3) \quad \frac{\mu}{q^3} \mathbf{q} = \alpha \mathbf{p} \times \mathbf{c}, \quad \mathbf{p} = \alpha \mathbf{c} \times \mathbf{q},$$

where $\alpha \neq 0$. Under our assumption the vectors \mathbf{q} and \mathbf{p} are not collinear. Taking the scalar product of both sides of the equations (5.3) with \mathbf{q} and \mathbf{p} , respectively, we obtain

$$\frac{\mu}{q} = \alpha c^2, \quad p^2 = \alpha c^2, \quad \mathbf{q} \cdot \mathbf{p} = 0.$$

The last condition implies that $c = qp$ and thus, from the second one we obtain $1 = \alpha q^2$. Using this, we can rewrite the first equation of (5.3) in the form

$$\frac{\mu}{q} \mathbf{q} = \mathbf{p} \times \mathbf{c}.$$

Comparing this with the definition (5.1) of the Laplace vector we see that $\mathbf{e} = \mathbf{0}$, i.e. the orbit is circular. Concluding, the integrals H and c^2 are dependent only in the cases of a circular or a straight line orbit.

5.2. Numerical results. For all tests we chose the orbit with $a = 1$, $e = 0.8$, $\Omega = \omega = \pi/2$, $i = \pi/4$, and we put $\mu = 4\pi^2$. For these values of μ and a the orbit period is one. The initial point was always located at the pericenter. After every hundred revolutions the results were stored. The equations of motion were integrated numerically over the time span of 10^5 by the Runge–Kutta procedure DOPRI with adaptive step-size control. This procedure implements the RK 5(4) algorithm of J. R. Dormand and P. J. Prince and can be found in the appendix to the book of Hairer *et al.* [42]. We translated the original FORTRAN code to Pascal. The influence of roundoff errors was minimized because we used the nineteen significant digit representation of floating point numbers (we used the extended type of Turbo Pascal). Local precision of integration was chosen to be 10^{-6} .

First tests with the simple observer and simple penalty methods applied to the integrals H and c^2 with $\theta_1 = 1$ and $\theta_2 = 1$ have shown that they cannot be used effectively for integration of the Kepler system. The step-size chosen by the integration procedure was very small (of order 10^{-10} after several revolutions for the observer method). This shows that the terms introduced by the simple observer and simple penalty methods are too big. There are two ways to overcome this difficulty. One can either decrease the values of θ_1 and θ_2 , or take the normalized observer and penalty methods. We chose the second possibility. We used the normalized observer method with $\alpha_1 = \alpha_2 = 1$ and $\beta_1 = \beta_2 = 1$ (see the definition of the normalized observer).

In our first test we compared the results obtained by DOPRI integration of Hamilton's equations for the Kepler system with those obtained by application of the normalized observer method to DOPRI integration of this problem. In Figure 9 the errors of the computed Hamiltonian are presented

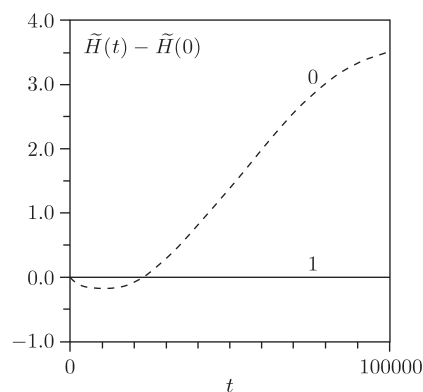


Fig. 9. Computed energy errors for the spatial Kepler problem over 100000 revolutions obtained by: (0) the DOPRI integrator and (1) the DOPRI integrator when the normalized observer method is applied to the integrals (H, c^2) .

as functions of time. Because the standard integration gives so bad results in further figures we do not include them.

Next, we compare the normalized observer method with: the normalized penalty method, the symplectic integration scheme of Yoshida (see [83], [46]), and finally with integration of the equations of motion regularized by the Kustaanheimo–Stiefel method which will be called briefly the K-S method (see [77]).

For the last method the original initial value problem is transformed to the form

$$(5.4) \quad \begin{cases} \frac{d\mathbf{u}}{ds} = \mathbf{v}, & \frac{d\mathbf{v}}{ds} = \frac{H}{2}\mathbf{u}, & \frac{dt}{ds} = \mathbf{u} \cdot \mathbf{u}, \\ \mathbf{u}(0) = \mathbf{u}_0, & \mathbf{v}(0) = \mathbf{v}_0, & t(0) = 0, \end{cases}$$

where $\mathbf{u}, \mathbf{v} \in \mathbb{R}^4$, t is the physical time, and

$$H = \frac{2\mathbf{v}_0 \cdot \mathbf{v}_0 - \mu}{\mathbf{u}_0 \cdot \mathbf{u}_0}.$$

The Cartesian coordinates \mathbf{q} can be expressed in terms of \mathbf{u} by the formula

$$\begin{pmatrix} q_1 \\ q_2 \\ q_3 \end{pmatrix} = \begin{pmatrix} u_1 & -u_2 & -u_3 & u_4 \\ u_2 & u_1 & -u_4 & -u_3 \\ u_3 & u_4 & u_1 & u_2 \end{pmatrix} \begin{pmatrix} u_1 \\ u_2 \\ u_3 \\ u_4 \end{pmatrix}.$$

For more details see [77].

Integration of the K-S system (5.4) shows that the DOPRI procedure chooses, for this system, a step-size too big for good preservation of integrals. Thus, for this integration the maximal step-size was limited to 0.01 while for other integrations it was equal to 1.

The step-size for the symplectic integrator was taken equal to 0.095 in order to have the computed energy error on the same level as in the normalized observer method. For this integration the results were stored after every 95 revolutions.

In Figure 10 the computed energy errors for all four methods are presented. Figures 11 and 12 show the errors in the computed first component of the Laplace vector and the errors in the position in the orbit, respectively. The last quantity is defined as the angle between the initial radius vector and the radius vector after some number of full revolutions:

$$\eta(nT) = \arccos \frac{\mathbf{q}(0) \cdot \mathbf{q}(nT)}{q(0)q(nT)}$$

where T denotes the period of the orbit and n is an integer.

Although we do not report all obtained results, from our computations it follows that the K-S method gives better results than the observer method only in the position in the orbit and in the argument of the pericenter.

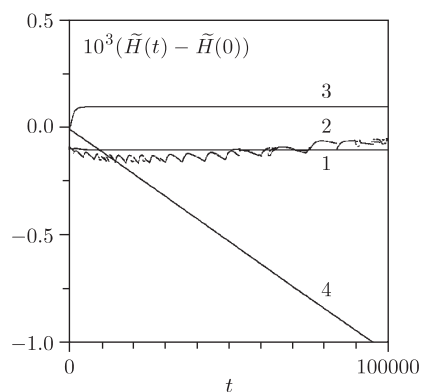


Fig. 10. The same as in Figure 9 obtained by: (1) the DOPRI integrator when the normalized observer method is applied to the integrals (H, c^2) , (2) the DOPRI integrator when the normalized penalty method is applied to the integrals (H, c^2) , (3) Yoshida's fourth order symplectic integrator and (4) the DOPRI integrator with the K-S regularized problem.

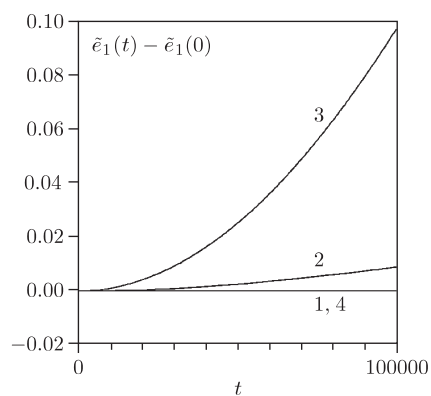


Fig. 11. Computed errors of the first component of the Laplace vector. Labels are as in Figure 10.

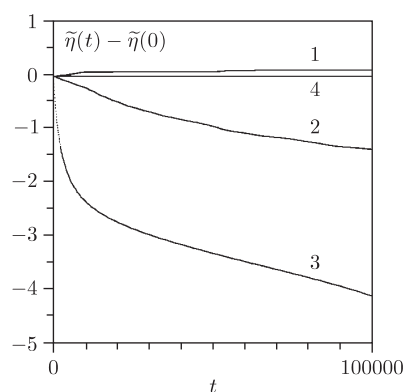


Fig. 12. Computed errors in the position in the orbit obtained by four integrators. Labels as in Figure 10.

However, it should be noted that in all cases the K-S method has a linear growth of errors.

Comparison of all results obtained for the symplectic integrator and the normalized observer shows that the latter is much more precise although the symplectic integrator is better in preservation of the components of the angular momentum. However, it should be noted that we used the observer method with only two integrals H and c^2 . Thus, one can expect that the use of the observer method applied to four integrals, H and the components of the Laplace vector \mathbf{e} , should improve the precision of the obtained results.

In our last test we checked the above hypothesis. We applied the normalized observer method to the integrals H and $\mathbf{c} = (c_1, c_2, c_3)$ with $\alpha_i = 10$,

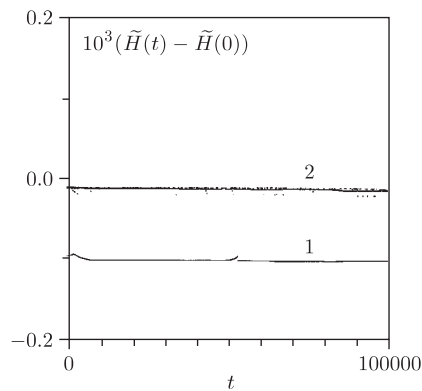


Fig. 13. Computed energy errors for the spatial Kepler problem over 100000 revolutions obtained by the DOPRI integrator with: (1) the normalized observer method applied to the integrals (H, c^2) and (2) the normalized observer applied to the integrals (H, c_1, c_2, c_3) .

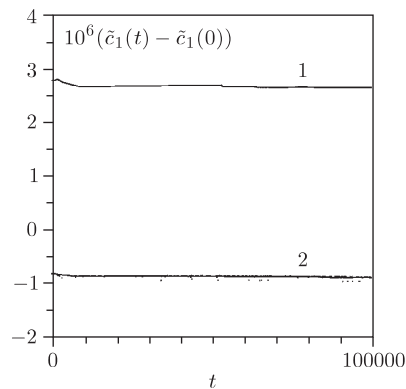


Fig. 14. Computed errors of the first component of the angular momentum for the spatial Kepler problem over 100000 revolutions obtained by the DOPRI integrator with: (1) the normalized observer method applied to the integrals (H, c^2) and (2) the normalized observer applied to the integrals (H, c_1, c_2, c_3) .

$1 \leq i \leq 4$, and $\beta_1 = \beta_3 = 10$, $\beta_2 = \beta_4 = 1$. Note that it is very important for the observer method to choose appropriate values of the constants: θ_i in the case of the simple observer and α_i, β_i in the case of the normalized observer. Especially in this last test it was difficult to find the “optimal” ones. Figures 13 and 14 show the errors in the energy and the first component of the angular momentum, respectively. Improvement of preservation of the angular momentum is not substantial and still the symplectic integrator gives better results for these quantities.

6. Gavrilov–Shil’nikov system

6.1. Description of the system. In this section we will consider a two-parameter family of Hamiltonian systems introduced by N. K. Gavrilov and L. P. Shil’nikov in [34].

These systems are defined on \mathbb{R}^4 and are given by the following Hamiltonian functions:

$$(6.1) \quad \begin{aligned} H &= H(x, \omega, \varepsilon), \quad x = (q_1, q_2, p_1, p_2) \in \mathbb{R}^4, \quad \omega, \varepsilon \in \mathbb{R}, \\ H &= \omega(q_1 p_2 - q_2 p_1) - \frac{\varepsilon}{2}(p_1^2 + p_2^2) + \frac{\varepsilon}{2}(q_1^2 + q_2^2) + \frac{\varepsilon}{4}(p_1^2 + p_2^2)^2. \end{aligned}$$

$x_0 = 0$ is the equilibrium point for this system. The type of the equilibrium depends on the sign of ε . For $\varepsilon < 0$, $\omega \neq 0$ it is a center-center point (i.e., the matrix of the linearized system has four purely imaginary eigenvalues). When $\varepsilon = 0$, $\omega \neq 0$ we have non-semisimple resonance of second order in our system (i.e., the matrix of the linearized system has two identical pairs of purely imaginary eigenvalues and it is not diagonalizable). Finally, for $\varepsilon > 0$, $\omega \neq 0$ it is a saddle-focus point and thus unstable (i.e., the matrix of the linearized system has four complex eigenvalues with non-zero real and imaginary parts).

The systems (6.1) are completely integrable. A second first integral is

$$K = q_1 p_2 - q_2 p_1.$$

Fix now $\varepsilon = 1$. The obtained system will be called briefly the G-S system.

For better understanding of the nature of the phase flow of our system let us introduce new canonical variables (with respect to the standard symplectic structure on \mathbb{R}^4):

$$(6.2) \quad \begin{cases} (q_1, q_2, p_1, p_2) \rightarrow (r, \phi, P, I), \\ q_1 = -P \cos \phi + \frac{I \sin \phi}{r}, & p_1 = r \cos \phi, \\ q_2 = -P \sin \phi - \frac{I \cos \phi}{r}, & p_2 = r \sin \phi. \end{cases}$$

Note that similar variables were introduced by Kovalev and Chudnenko ([47]) who studied stability conditions of an equilibrium point in a Hamil-

tonian system with two degrees of freedom in the case of non-semisimple resonance of second order (see also [76] and the formula (11) on p. 262 in [3]).

In the new variables the Hamiltonian (6.1) has the form

$$H(r, \phi, P, I) = \omega I - \frac{1}{2}r^2 + \frac{1}{2}\left(P^2 + \frac{I^2}{r^2}\right) + \frac{1}{4}r^4.$$

The coordinate ϕ is cyclic and, as a consequence, $I = K$ is a first integral. This allows us to reduce our system to one degree of freedom. The Hamiltonian of the reduced system is

$$(6.3) \quad H_R(r, P) = \frac{1}{2}\left(P^2 - r^2 + \frac{I^2}{r^2}\right) + \frac{1}{4}r^4.$$

The level sets $H_R = \text{const}$ define phase curves of the reduced system on the (r, P) -plane. Because

$$\frac{d\phi}{dt} = \frac{\partial H}{\partial I} = \omega + \frac{I}{r^2},$$

when $\omega \neq 0$, $d\phi/dt$ has a constant sign for sufficiently small $|I|$, and so these level curves can be interpreted as the closure of the traces of the orbits of the original system defined by the Hamiltonian (6.3) on the Poincaré surface of section $\phi = 0 \pmod{2\pi}$ at least when these orbits are not periodic. Figures 15(a) and 15(b) show these levels for $I = 0$ and $I = 0.1$, respectively. In the first of these figures we can see that there exists a “figure 8” homoclinic loop for the reduced system. This can be easily shown analytically. Thus in the G-S system, the stable and unstable manifolds of the equilibrium have

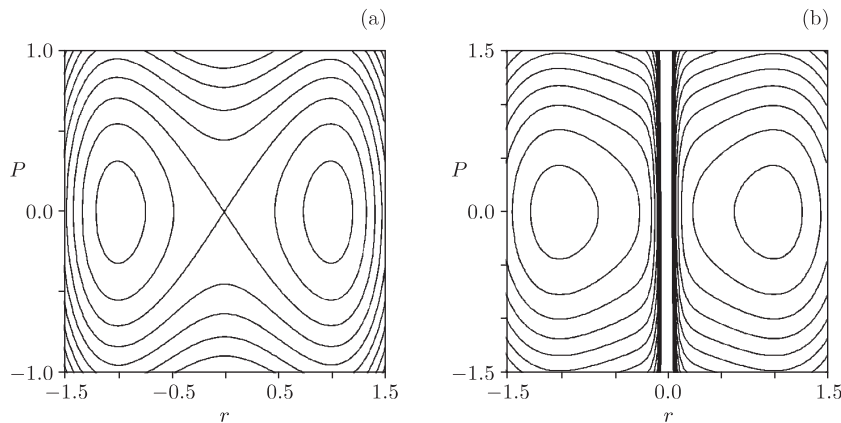


Fig. 15. Constant value levels of the G-S reduced Hamiltonian (6.3) for: (a) $I = 0$ (the contours correspond to $H_R = -0.3 + 0.1k$, $k = 1, 2, \dots$; the smallest ovals correspond to the minimal value of H_R) and (b) $I = 0.1$ (the contours correspond to $H_R = -0.35 + 0.2k$, $k = 1, 2, \dots$).

a common point. Because $\omega \neq 0$, the equilibrium point is of saddle-focus type. Consequently, as the system is integrable, these manifolds coincide.

N. K. Gavrilov and L. P. Shil'nikov introduced the systems described above in their investigations of the phenomenon of changing stability type of an isolated equilibrium in a general one-parameter family of Hamiltonian systems with two degrees of freedom.

We found this system challenging for testing precision of numerical integration. Every numerical procedure “disturbs” the original system in some way. As was shown by L. M. Lerman and Ya. L. Umanskiĭ in [53] small perturbations of an integrable two-degrees-of-freedom Hamiltonian system with a saddle-focus equilibrium point cause, typically, splitting of the asymptotic surfaces, appearance of a transversal homoclinic orbit, and thus non-integrability (see [25]). Thus, one can expect that any numerical procedure should produce “numerical chaos” for the G-S system in a neighbourhood of the equilibrium point $x_0 = 0$ on the $H = K = 0$ level. Note that this level set is compact and that on it the integrals H and K are dependent at $x_0 = 0$.

6.2. Numerical results. For numerical experiments we put $\omega = 2\pi$. In all cases presented below the equations of motion corresponding to the Hamiltonian (6.1) were integrated numerically. We applied the general extrapolating code for solving ODE's from [42]. The original FORTRAN procedure ODEX was translated into Pascal. The influence of roundoff errors on our results is minimal because we used nineteen-significant-digits representation of floating numbers (the extended type of Turbo Pascal v.6.0 of Borland International). Local precision of integration was 10^{-14} . The results are presented on the Poincaré surface of section $\{p_1 = 0, p_2 > 0\}$, on the constant energy surface $H = 0$ which contains our equilibrium point. Position of points on the section was determined with precision higher than 10^{-15} . We always stopped integrations after obtaining 10000 points.

In every test we integrated the equations of motion with the initial condition $(0, 0, 0, \sqrt{2})$. This point lies on the homoclinic loop. Thus, theoretically we should obtain a sequence of points lying on one half of the homoclinic loop and approaching asymptotically the equilibrium point. However, in practice, because of numerical errors, the computed orbit passes near the equilibrium and we obtain a sequence of points that lie near the entire homoclinic loop.

First, the original Hamilton equations of motion corresponding to the Hamiltonian (6.1) were integrated. Figure 16 shows, on the surface of section, the obtained homoclinic loop. In Figure 17 the magnification of the neighbourhood of the equilibrium is presented. Our suggestion that in the G-S system numerical chaos is generated is fully confirmed. We obtained qualitatively similar results when Merson's fourth order Runge–Kutta method (see Chapter 2 of [42]) was used for integration.

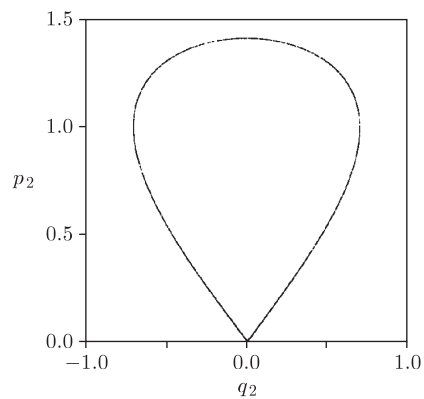


Fig. 16. The trace on the surface of section of the orbit homoclinic to the equilibrium point $x_0 = 0$ of the G-S system computed without the observer method.

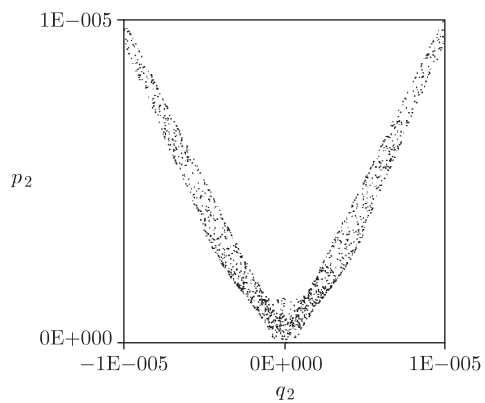


Fig. 17. Magnification of the neighbourhood of the equilibrium point from Figure 16.

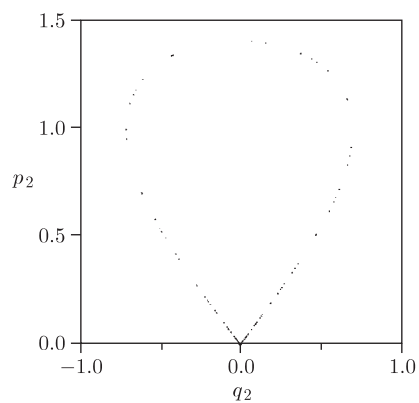


Fig. 18. The same as in Figure 16 when the simple observer method is applied to the integrals (H, K) .

Next, we integrated the equations of motion of the G-S system with the simple observer applied to both integrals H and K and with $\theta_1 = \theta_2 = 10$. The obtained homoclinic loop is shown in Figure 18. Notice the difference between Figures 16 and 18. During the integration with the observer perturbations the computed orbit goes only few times along the homoclinic loop, and after that it oscillates very close to the equilibrium point. As a result almost 90% points in Figure 18 lie in a very small neighbourhood of the equilibrium point. Moreover, two different magnifications of the neighbourhood presented in Figures 19(a) and 19(b) show that numerical chaos disappeared.

We also applied the simple observer method to the integral H only with $\theta = 0.2$. In Figure 20 the obtained results are presented. Comparison with

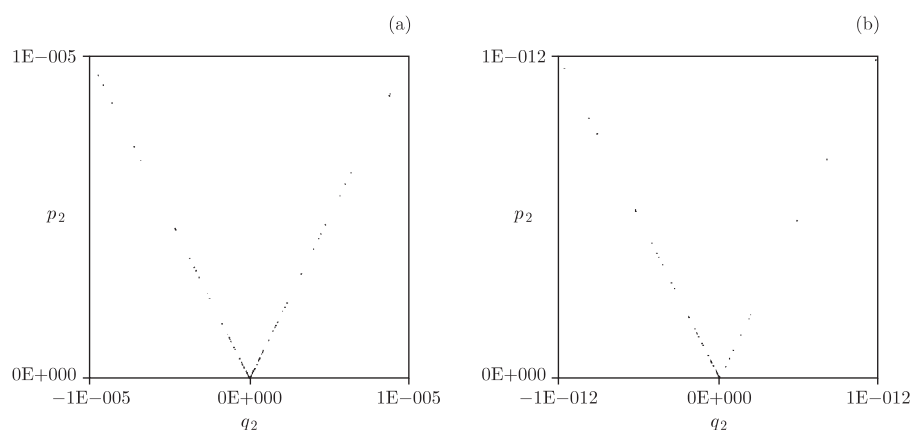


Fig. 19. Two magnifications of the neighbourhood of the equilibrium point from Figure 18.

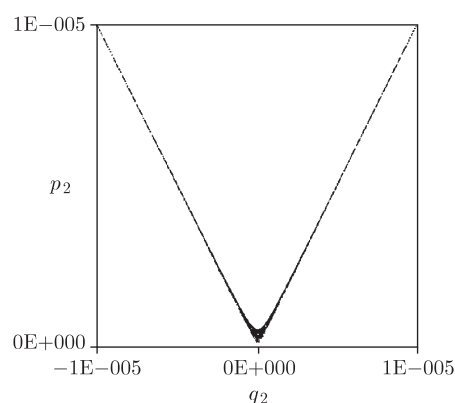


Fig. 20. The same as in Figure 17 when the simple observer method is applied only to the integral H .

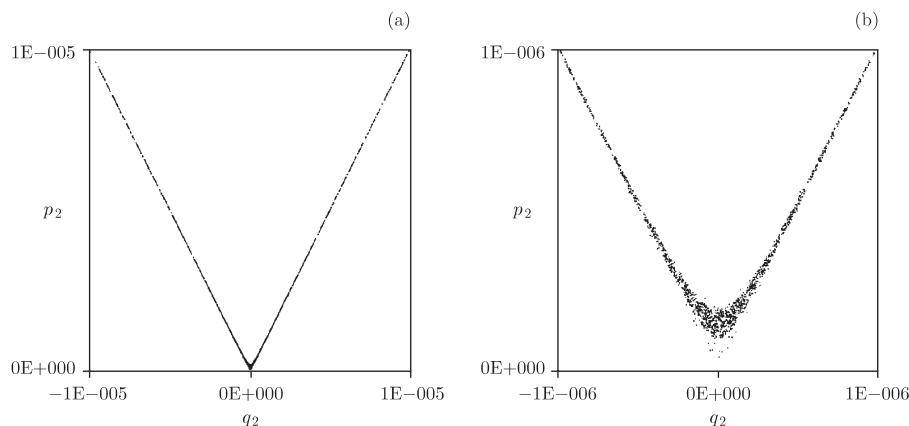


Fig. 21. Two magnifications of the neighbourhood of the equilibrium point when the simple penalty method is applied to the two integrals (H, K).

Figure 19(a) clearly shows that the chaotic region does not disappear. However, it is confined to the vicinity of the homoclinic loop.

Finally, the simple penalty method was applied to both integrals H and K with $\theta_1 = \theta_2 = 10$. In Figures 21(a) and 21(b), as in Figures 19 and 20, magnifications of the neighbourhood of the equilibrium point are presented. Notice that the chaotic region also appears but it is very thin.

In our next tests, we compared the simple observer method with a symplectic integrator. For symplectic integration we chose Butcher's fourth order implicit Runge–Kutta method ([21]). The fact that the Butcher method is symplectic is discussed in [72].

First, we integrated the original equations of motion of the G-S system with the simple observer applied to both integrals using Merson's fourth order Runge–Kutta method. The fixed step-size was chosen equal to 0.01 and we put $\theta_1 = \theta_2 = 10$. The initial condition was the same as in the previous tests. The results are presented in Figures 22(a)–(d). In Figure 22(a) we can see that the numerically computed orbit approaches asymptotically the equilibrium point. This is fully confirmed in Figures 22(b), (c), (d) where magnifications of the neighbourhood of the equilibrium point are shown. In these figures, one side of the neighbourhood is only shown because there are no points with $q_2 < 0$. Thus, these results coincide with the theoretical predictions. We noticed that during numerical computation when the orbit approaches the equilibrium, the errors of both integrals decrease rapidly. After obtaining 100 points on the cross section, the errors of both integrals are practically zero.

Here it should be explained why the, potentially better, integrator ODEX gave worse results than the fixed step-size Runge–Kutta method (compare Figures 18 and 22). It was checked that the procedure ODEX is too “liberal”

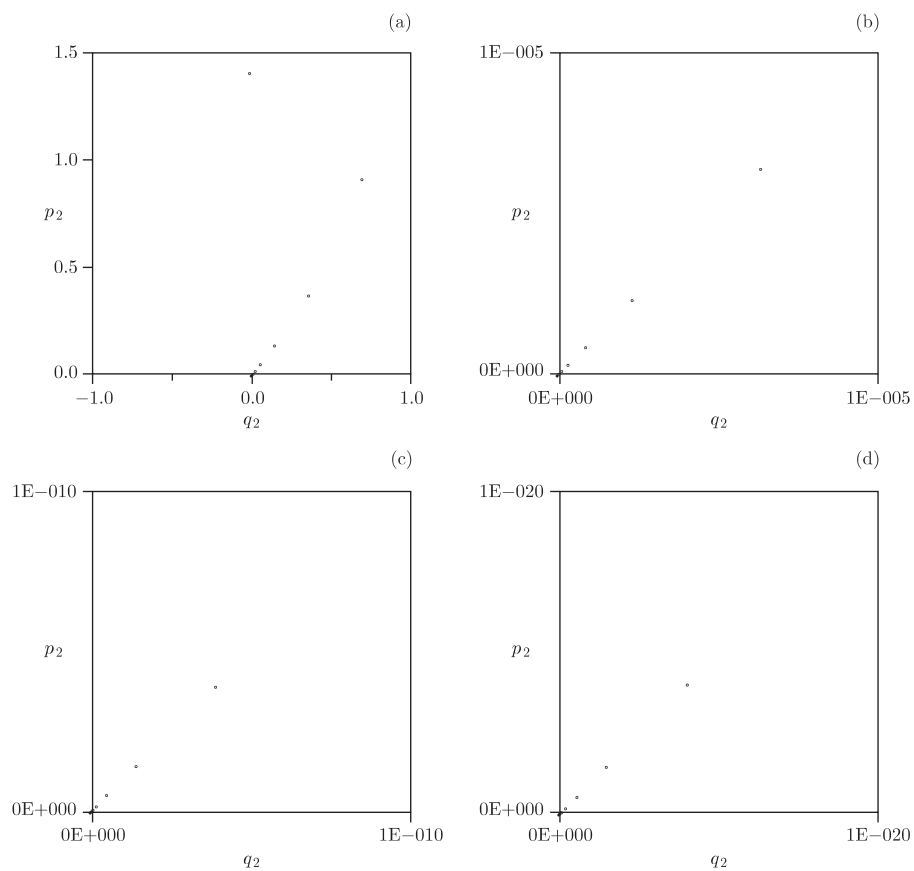


Fig. 22. (a) The trace on the surface of section of the orbit homoclinic to the equilibrium point $x_0 = 0$ of the G-S system computed by Merson's Runge-Kutta method with the simple observer method applied to the integrals (H, K) . (b)-(d) Successive magnifications of the neighbourhood of the equilibrium point for (a).

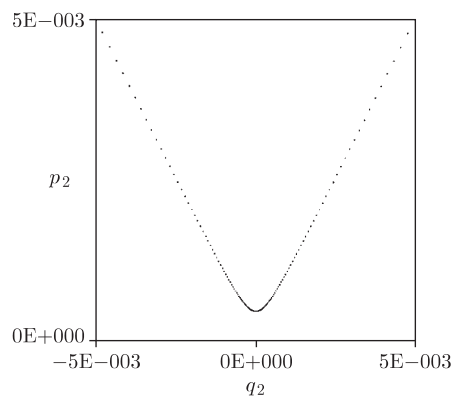


Fig. 23. Magnifications of the neighbourhood of the equilibrium point when the homoclinic orbit was computed by Butcher's fourth order symplectic integrator.

in choosing a step of integration. When the maximal allowed step-size was limited to 0.1, integration with the ODEX procedure gave results similar to those obtained by the Runge–Kutta method.

Next, we integrated the G-S system using Butcher’s symplectic method with step-size 0.01. The results are presented in Figure 23. Notice that the computed orbit goes quite far from the equilibrium point. However, Butcher’s method has an excellent property: it does not produce “numerical chaos” in the G-S system. We checked this choosing different initial conditions on the homoclinic loop. Even if we start integration from a point lying at a distance of order 10^{-17} from the equilibrium point the computed orbit lies close to the homoclinic loop, but “numerical chaos” is undetectable. This very good behaviour of the symplectic integrator can perhaps be explained by the fact that the G-S system is relatively simple: one of its integrals is quadratic and two of the equations of motion are linear (see e.g. [72]).

In order to compare the observer method and the symplectic integrator on a more complicated system we introduced a modified G-S system with the following Hamiltonian:

$$H = \omega(q_1 p_2 - q_2 p_1) - \frac{1}{2}(p_1^2 + p_2^2) + \frac{1}{2}(q_1^2 + q_2^2) \\ + \frac{1}{2}(p_1^2 + p_2^2) \left\{ \frac{1}{2}(p_1^2 + p_2^2) + A(q_1 p_2 - q_2 p_1) + B(q_1^2 + q_2^2) \right\}$$

where ω , A , B are real parameters. Note that we add to the Hamiltonian (6.1) of the G-S system two fourth order terms, thus the type of the equilibrium point in the new system is the same as in the G-S system. Moreover, using the canonical transformation (6.2) we can easily prove that the modified G-S system is integrable with the same second integral K and that it possesses, for $B > -1$, the “figure 8” homoclinic loop on the (r, P) plane.

For tests we chose $A = 0.2$, $B = -0.2$, $\omega = 2\pi$ and the step-size $h = 0.01$. The initial condition was $(0, -P, 0, r)$ with $r = 10^{-10}$ and

$$P = r \sqrt{\frac{2 - r^2}{2(1 + Br^2)}}.$$

This point lies on the homoclinic loop at a distance of approximately 10^{-10} from the equilibrium point. The orbit with this initial condition for $t \rightarrow +\infty$ goes along the whole loop and asymptotically approaches the equilibrium point from the positive side of the q_2 -axis.

Using Merson’s Runge–Kutta method we integrated the equations of the modified G-S system with the simple observer method applied to both integrals, and $\theta_1 = \theta_2 = 10$. The results are presented in Figure 24(a). The series of magnifications of the neighbourhood of the equilibrium point (see Figures 24(b), (c), (d)) shows that the computed orbit behaves exactly as the theory predicts.

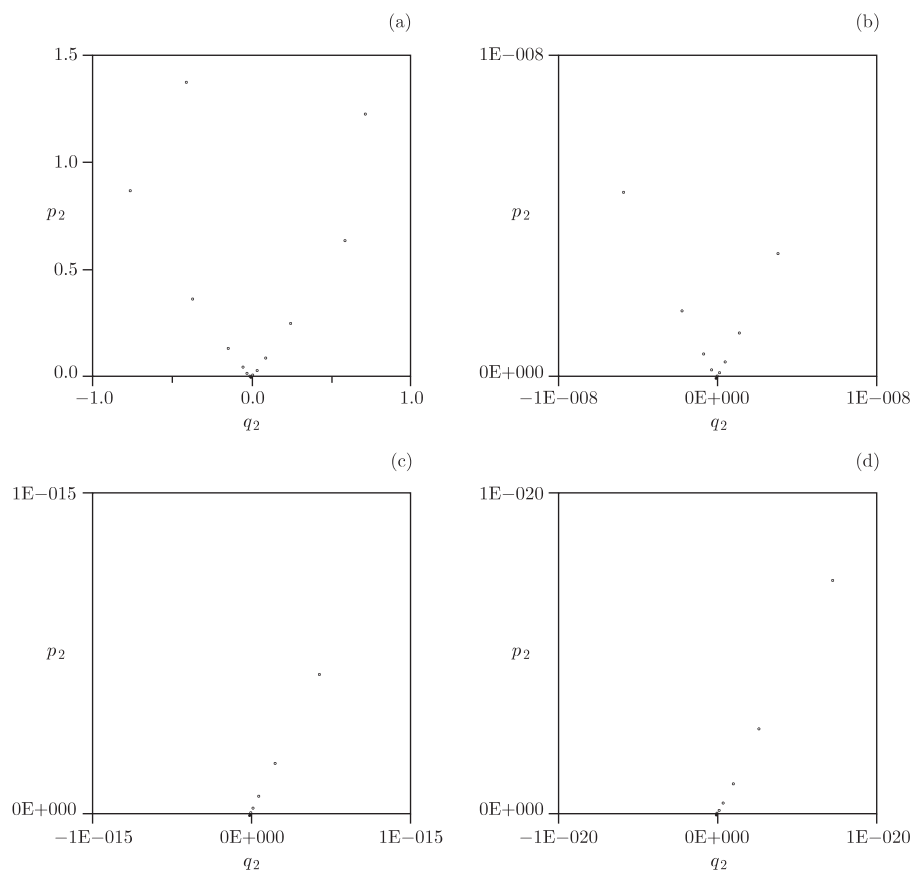


Fig. 24. The same as in Figure 22 for the modified G-S system.

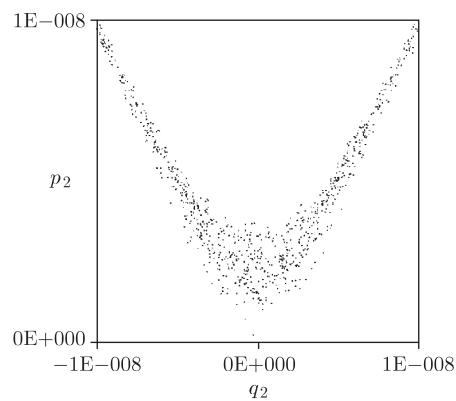


Fig. 25. The same as in Figure 23 for the modified G-S system.

Symplectic integration with Butcher's method gives the results presented in Figure 25. We can see that for the modified G-S system the symplectic

integrator generates “numerical chaos” although it is located in a very thin layer around the homoclinic loop.

The extremely good coincidence between the theoretically predicted and numerically computed orbits of our system clearly indicates that here the use of the observer method increases the reliability of numerical computations.

7. The Euler equations on the Lie algebra $so(4)$

7.1. Description of the system. The general theory of the Euler equations on Lie algebras can be found in [11], [32], [33], [63], [65]–[70], [80]. The specific case of the Euler equations on the Lie algebra $so(4)$ is studied in more detail in [1], [40], [80] and [82]. Because these equations are used here exclusively as an interesting and non-trivial example of application of the observer method, we write them down directly without any explanation of their Lie algebraic origin.

Let us fix real numbers $\{\lambda_i\}_{1 \leq i \leq 6}$ and consider the system of six ODE’s:

$$(7.1) \quad \begin{cases} \frac{dx_1}{dt} = (\lambda_3 - \lambda_2)x_2x_3 + (\lambda_6 - \lambda_5)x_5x_6, \\ \frac{dx_2}{dt} = (\lambda_1 - \lambda_3)x_1x_3 + (\lambda_4 - \lambda_6)x_4x_6, \\ \frac{dx_3}{dt} = (\lambda_2 - \lambda_1)x_1x_2 + (\lambda_5 - \lambda_4)x_4x_5, \\ \frac{dx_4}{dt} = (\lambda_3 - \lambda_5)x_3x_5 + (\lambda_6 - \lambda_2)x_2x_6, \\ \frac{dx_5}{dt} = (\lambda_4 - \lambda_3)x_3x_4 + (\lambda_1 - \lambda_6)x_1x_6, \\ \frac{dx_6}{dt} = (\lambda_2 - \lambda_4)x_2x_4 + (\lambda_5 - \lambda_1)x_1x_5. \end{cases}$$

This is the system of Euler equations on the Lie algebra $so(4)$ corresponding to the “Hamiltonian” $\frac{1}{2} \sum_{i=1}^6 \lambda_i x_i^2$.

It always admits the following three first integrals:

$$(7.2) \quad \begin{cases} H_1 = x_1x_4 + x_2x_5 + x_3x_6, \\ H_2 = \sum_{i=1}^6 x_i^2, \\ H_3 = \sum_{i=1}^6 \lambda_i x_i^2. \end{cases}$$

When $\{\lambda_i\}_{1 \leq i \leq 6}$ are not all equal, these three integrals are functionally independent.

The integrals H_1 and H_2 are intimately related to the Lie algebra $so(4)$, they represent its ‘‘Casimir functions’’.

To be integrable (see Section 28 of [2]), the system (7.1) must have a fourth first integral H_4 , functionally independent of H_1, H_2, H_3 . Suppose that $\lambda_i = \lambda_j$ for at most two pairs $\{i, j\}$, $i \neq j$. Then the unique known case when such a fourth first integral exists is the so-called *Manakov case*, defined by the condition

$$\lambda_1 \lambda_4 (\lambda_2 + \lambda_5 - \lambda_3 - \lambda_6) + \lambda_2 \lambda_5 (\lambda_3 + \lambda_6 - \lambda_1 - \lambda_4) + \lambda_3 \lambda_6 (\lambda_1 + \lambda_4 - \lambda_2 - \lambda_5) = 0.$$

In this case one can take

$$H_4 = a_1 x_1^2 + a_2 x_2^2 + a_3 x_3^2 + a_4 x_4^2 + a_5 x_5^2 + a_6 x_6^2,$$

with appropriate constants $\{a_i\}_{1 \leq i \leq 6}$ (see [1]).

One can prove that, under our assumption concerning the $\{\lambda_i\}_{1 \leq i \leq 6}$, except for the Manakov case, the system (7.1) is never algebraically completely integrable (see [1], [40], [41]).

Our main aim is to obtain a reliable graphical representation of the behaviour of the orbits of (7.1). As usual, we will use the Poincaré surface of section.

For $\{\lambda_i\}_{1 \leq i \leq 6}$ fixed, define

$$M(h_1, h_2, h_3) = \{x \in \mathbb{R}^6 : H_1(x) = h_1, H_2(x) = h_2, H_3(x) = h_3\},$$

where $x = (x_1, \dots, x_6)$.

Typically $M(a, b, c)$, when non-empty, is a compact, smooth, three-dimensional submanifold of \mathbb{R}^6 , filled with orbits of the system (7.1).

In what follows we will concentrate on a particular non-Manakov case:

$$(7.3) \quad \lambda_1 = 1, \quad \lambda_2 = 5, \quad \lambda_3 = 2, \quad \lambda_4 = 1, \quad \lambda_5 = 3, \quad \lambda_6 = 4,$$

and

$$(7.4) \quad h_1 = 1, \quad h_2 = 15, \quad h_3 = 25.$$

Let us underline that this choice of values of the parameters is largely fortuitous except for the fact that $\lambda_1 = \lambda_4 = 1$ and $h_2 < h_3$; indeed, the last two conditions will play an essential role in the determination of our surface of section.

Now, let us describe it. Consider the two-dimensional manifold

$$\widetilde{M}(h_1, h_2, h_3) = \{x \in M(h_1, h_2, h_3) : x_3 = 0\}.$$

We would like to choose $\widetilde{M}(h_1, h_2, h_3)$ as our surface of section. Unfortunately it is not clear how to choose the global coordinate system on it. Therefore we proceed as follows.

Consider a point $X = (x_1, 0, x_3, x_4, x_5, x_6) \in \widetilde{M}(h_1, h_2, h_3)$ and count how many points of $\widetilde{M}(h_1, h_2, h_3)$ have the same fifth and sixth coordinates as X .

From (7.2)–(7.4) one gets

$$(7.5) \quad x_3 = \varepsilon \sqrt{h_3 - h_2 - 2x_5^2 - 3x_6^2},$$

where $\varepsilon = \pm 1$. On the other hand, from (7.2) one obtains

$$(7.6) \quad x_1 x_4 = h_1 - x_3 x_6 \stackrel{\text{def}}{=} P_\varepsilon,$$

and

$$(7.7) \quad x_1^2 + x_4^2 = h_2 - x_3^2 - x_5^2 - x_6^2 \stackrel{\text{def}}{=} S,$$

where x_3 is the same as in (7.5) and the sign of ε in (7.6) is the same as in (7.5). Finally, from (7.6) and (7.7) one deduces that

$$x_1 + x_4 = \eta \sqrt{S + 2P_\varepsilon},$$

where $\eta = \pm 1$, and that

$$x_1 - x_4 = \theta \sqrt{S - 2P_\varepsilon},$$

where $\theta = \pm 1$.

Thus, when x_5 and x_6 are fixed, we have at most eight different points in $\widetilde{M}(h_1, h_2, h_3)$ with these particular x_5 and x_6 as fifth and sixth coordinate. Consequently, we can cover $\widetilde{M}(h_1, h_2, h_3)$ with eight charts defined by the choice of ε , η and θ , i.e. by fixing the sign of x_3 , $x_1 + x_4$ and $x_1 - x_4$. In any of such charts, (x_5, x_6) is a global coordinate system.

These charts, denoted by $\{\Gamma_i\}_{1 \leq i \leq 8}$, are defined as follows:

	Γ_1	Γ_2	Γ_3	Γ_4	Γ_5	Γ_6	Γ_7	Γ_8
ε	–	–	–	–	+	+	+	+
η	–	–	+	+	–	–	+	+
θ	–	+	–	+	–	+	–	+

7.2. Numerical results. First we will study the non-Manakov case defined by (7.3). In this case the system (7.1) was integrated by the RKF method (see Section 4.1) with the simple observer, where $\theta_1 = \theta_2 = \theta_3 = 10$. The control error was $5 \cdot 10^{-8}$. The integration time was approximately 400000. All computations in this section were done on the same computer as in Section 4.

In Figure 26(a) one can find the trace of one chaotic orbit on Γ_1 , computed by the above method. We verified that the shape of the obtained chaotic region is independent of the chosen initial orbit, by tracing the similar figures for many different orbits passing through the chaotic region of Figure 26(a).

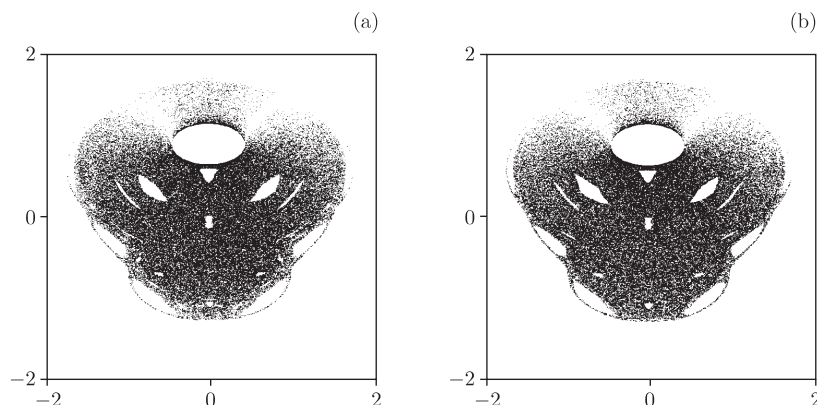


Fig. 26. The chaotic region on the chart Γ_1 obtained as the trace of one chaotic orbit computed by: (a) the RKF method with the simple observer method applied to the first integrals (H_1, H_2, H_3) and (b) the Lie–Poisson integrator. There are 140858 and 146221 points in figures (a) and (b) respectively.

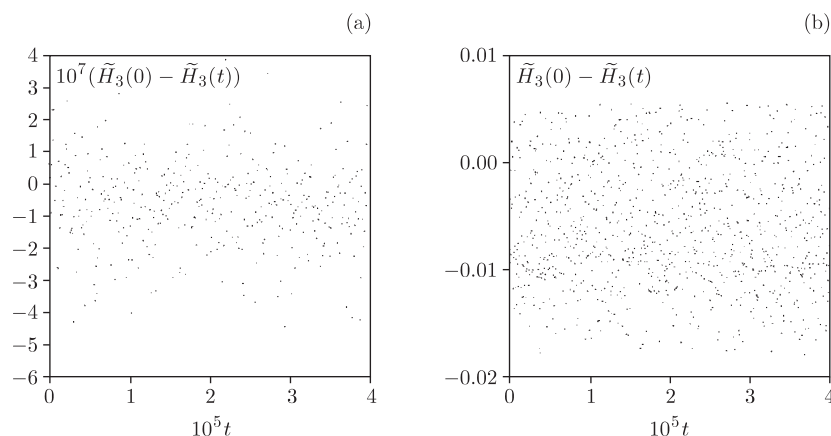


Fig. 27. Error in the computed first integral \tilde{H}_3 obtained by: (a) the RKF method with the simple observer method applied to the first integrals (H_1, H_2, H_3) and (b) the Lie–Poisson integrator.

The system (7.1) can also be integrated by the so-called Lie–Poisson integrators ([35]) which generalize the symplectic methods to the case of Hamiltonian equations on Lie algebras.

In [62] the Lie–Poisson integration scheme of Ge Zhong and J. E. Marsden ([35]) in the form given by P. J. Channell and J. C. Scovel ([22]) was applied to integrate the system (7.1) with $\{\lambda_i\}_{1 \leq i \leq 6}$ as above. More precisely, the integration step $1/400$ and precision 10^{-13} were used, with integration time 400000. Figure 26(b) (from [62]) was obtained exactly as Figure 26(a) but with the use of this integration scheme (see [62] for more details).

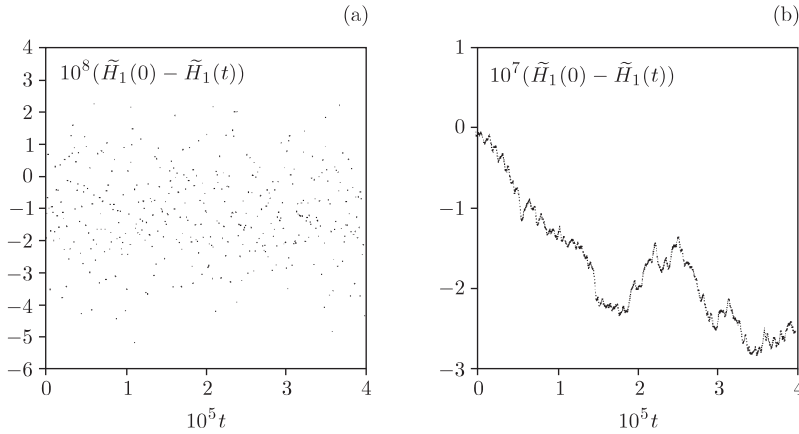


Fig. 28. The same as in Figure 27 but for the computed first integral \tilde{H}_1 .

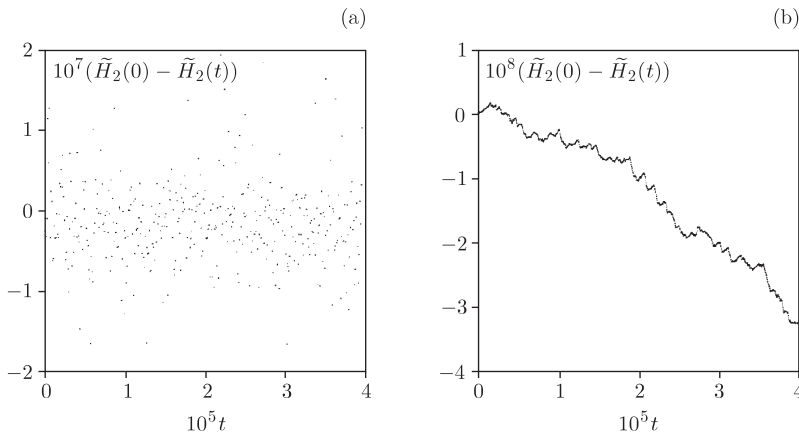


Fig. 29. The same as in Figure 27 but for the computed first integral \tilde{H}_2 .

The resemblance between both figures is exceptionally good. This is an argument in favour of the reliability of our computations.

Let us now see how the computed first integrals H_1 , H_2 and H_3 are preserved.

One can see (Figures 27(a), (b)) that the Hamiltonian H_3 is much better preserved by the RKF method with the simple observer than by the Lie–Poisson integration scheme. The errors on the remaining integrals H_1 and H_2 are comparable (see Figures 28(a), (b) and Figures 29(a), (b)). Nevertheless, the error in the RKF method with the simple observer is oscillating around a stable non-zero value (see the remark at the end of Section 3) while the error in the Lie–Poisson integration scheme increases for H_1 and H_2 . Figures 27(b), 28(b) and 29(b) are taken from [62].

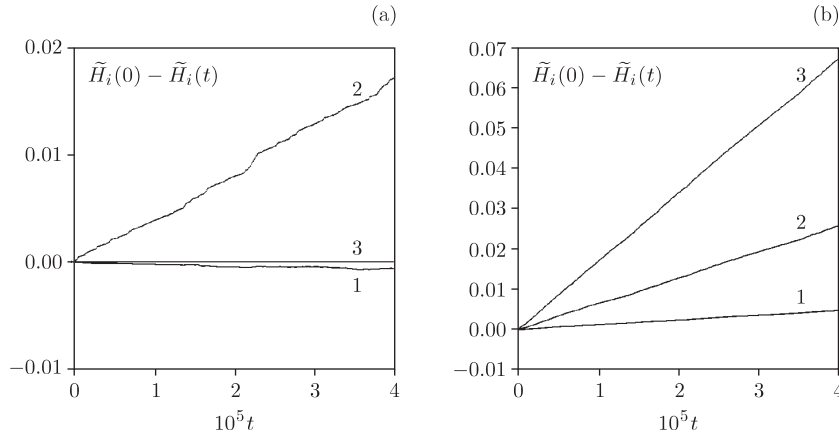


Fig. 30. Errors in the computed first integrals $(\tilde{H}_1, \tilde{H}_2, \tilde{H}_3)$ obtained by: (a) the RKF method with the simple observer method applied only to the Hamiltonian H_3 and (b) the RKF method without the observer method. The three curves correspond to $i = 1, 2$ and 3 , respectively.

Finally, let us compare the behaviour of the computed first integrals H_1 , H_2 and H_3 when the observer method is applied to some of them. More precisely, we use the simple observer method only in order to preserve H_3 (the Hamiltonian of the system) and we plot the behaviour of the error for all first integrals. As one can see in Figure 30(a), the Hamiltonian H_3 is well preserved but moreover, H_1 and H_2 are quite well preserved too. Moreover, H_1 and H_2 are better preserved than without the use of the observer method on H_3 (see Figure 30(b)). This confirms the fact that the use of the observer method increases the reliability of computations.

8. An example of an Anosov flow

8.1. Description of the system. This section is inspired by Section 3.2 of [22]. It is well known that among smooth dynamical systems with continuous time and compact phase space, the Anosov flows have the most chaotic behaviour, enjoying the strongest possible ergodic properties ([73]).

The simplest and oldest examples of Anosov flows are provided by the geodesic flows on compact orientable surfaces M^2 having constant negative curvature -1 (see [73], [24]).

Let M^2 be a compact orientable two-dimensional Riemannian manifold (surface) of constant negative curvature -1 .

Let us consider the open unit disc

$$D^2 = \{(q_1, q_2) \in \mathbb{R}^2 : q_1^2 + q_2^2 < 1\}$$

equipped with the non-Euclidean Riemannian metric

$$(8.1) \quad \frac{dq_1^2 + dq_2^2}{(1 - q_1^2 - q_2^2)^2}$$

of constant negative curvature -1 (see Chapter 2 of [26]).

It is well known that any surface M^2 as above is isometric to the quotient space \mathbf{D}^2/Γ , where Γ is a discrete subgroup of the homographic transformations group acting on the unit disc \mathbf{D}^2 (see Chapter 4 of [27]).

The geodesics on M^2 can be obtained as projections on \mathbf{D}^2/Γ of the geodesics on \mathbf{D}^2 corresponding to the Riemannian metric (8.1).

The geodesic flow on \mathbf{D}^2 is governed by the Hamiltonian

$$(8.2) \quad H(q, p) = \frac{(1 - q_1^2 - q_2^2)^2(p_1^2 + p_2^2)}{4},$$

where $q = (q_1, q_2) \in \mathbf{D}^2$, $p = (p_1, p_2) \in \mathbb{R}^2$.

From now on let us consider the particular case when M^2 is a doughnut with two holes, i.e. a compact orientable surface of genus 2 equipped with the non-Euclidean metric of constant curvature -1 .

In [27] one can find the explicit description of the discrete groups Γ of homographies of the unit disc \mathbf{D}^2 such that $M^2 = \mathbf{D}^2/\Gamma$, as well as of the fundamental region $\Omega \subset \mathbf{D}^2$ of the subgroup Γ which was used by Channell and Scovel ([22]) and which we will also use here.

The boundary of the fundamental region Ω is a piecewise smooth curve L defined as follows.

Let

$$R_0 = \frac{\sin \beta}{\cos \beta + \sqrt{\cos 2\beta}} \approx 0.21684534 \dots$$

with $\beta = \pi/8$. Inside the octant $\Pi_1 = \{(q_1, q_2) \in \mathbf{D}^2 : 0 \leq |q_2| \leq q_1 \tan \beta\}$ the boundary curve is defined by the equation

$$1 + q_1^2 + q_2^2 - 2q_1 \frac{1 + R_0^2}{1 - R_0^2} = 0.$$

The boundary in the other octants is obtained by rotation by a multiple of $\pi/4$ (see Figure 31).

For every point $q \in \mathbf{D}^2$ there exists a homographic transformation $\gamma \in \Gamma$ such that $\gamma(q) \in \Omega$. If $\gamma(q) \in \Omega \setminus L$, then such a γ is unique.

For $q \in \Pi_1 \setminus \Omega$, but belonging to a thin layer around L , the corresponding homographic transformation γ , $\gamma(q_1 + iq_2) = \bar{q}_1 + i\bar{q}_2$, is of the form

$$(8.3) \quad \begin{cases} \bar{q}_1 = \frac{ab(q_1^2 + q_2^2) + q_1(a^2 + b^2) + ab}{b^2(q_1^2 + q_2^2) + 2abq_1 + a^2}, \\ \bar{q}_2 = \frac{q_2(a^2 - b^2)}{b^2(q_1^2 + q_2^2) + 2abq_1 + a^2}, \end{cases}$$

where $a = 1 + 1/R_0^2$ and $b = 1 - 1/R_0^2$. Similar transformations in the other octants are obtained from (8.3) by rotation by a multiple of $\pi/4$.

Any such mapping induces in a natural way a mapping of momenta by

$$(8.4) \quad \bar{p} = (D_\gamma^T(q))^{-1}p$$

where $D_\gamma^T(q)$ is the transposed of the Jacobian matrix of the mapping γ at q .

8.2. Numerical results. The Hamiltonian (8.2) written down in Section 3.2 of [22] was used there for the numerical study of the geodesic flow on a doughnut with two holes. This study was done with the use of the symplectic integrator of order 4. But the final result concerning the preservation of the computed Hamiltonian \tilde{H} was, in the opinion of the authors of [22], not completely satisfactory. They suggested that the very strong ergodic properties of the system under consideration prevent really good numerical results, independently of the method used.

We will now show, applying exactly the same geometrical machinery as in [22], that the use of a standard Runge–Kutta integration procedure with the simple observer method allows us to obtain results substantially better than those reported by Channell and Scovel.

We choose at random a point $q_0 \in \Omega$ and a vector $p_0 \in \mathbb{R}^2$. We compute numerically the piece of the orbit of the phase flow governed by the Hamiltonian (8.2) up to the first computed point (q, p) such that $q \notin \Omega$. Then, using the formulae (8.3) and (8.4), we obtain the point (\bar{q}, \bar{p}) where $\bar{q} \in \Omega$ and we continue our computations as before. Note that on M^2 the projections of q and \bar{q} are almost the same.

The pieces of orbits in Ω obtained in this way represent the computed geodesic line on M^2 passing through q_0 in the direction p_0 .

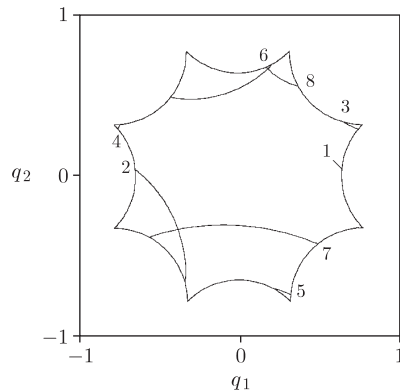


Fig. 31. A piece of a geodesic on M^2 . Numbers mark successive origins of smooth pieces of the geodesic.

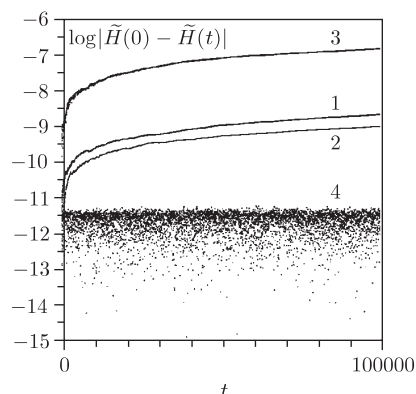


Fig. 32. Errors in the computed Hamiltonian for the geodesic flow on M^2 obtained by: (1) Merson's Runge–Kutta method, (2) Butcher's fourth order symplectic method, (3) fourth order generating function symplectic integrator and (4) Merson's Runge–Kutta method with the simple observer method.

In Figure 31 one can find a piece of such a geodesic on M^2 represented in this way inside Ω . In Figure 32 the errors of the computed Hamiltonian for four integrations with the fixed step-size $h = 0.01$ are presented. We integrated the equations of motion using Merson's Runge–Kutta method, Merson's Runge–Kutta method with the simple observer, Butcher's fourth order symplectic Runge–Kutta method and fourth order generating function integrator described in [22], respectively. The advantage of the application of the observer method clearly appears.

Acknowledgments. The fourth author thanks Dr. S. Wojciechowski from Department of Mathematics of Linköping Institute of Technology (Sweden), who many years ago introduced him to the world of Euler equations, and Dr. M. Balabane from Department of Mathematics of University Paris-Nord (France) for discussions on the observer method and his idea of the penalty method.

We thank O. Neron de Surgy from l'Observatoire de Paris for his kind permission to reproduce figures from [62].

We also thank Dr. M. Lemańczyk from Department of Mathematics of Toruń University (Poland), Dr. T. Nadzieja from Department of Mathematics of University of Wrocław (Poland) and Dr. C. Simó from Department of Applied Mathematics of University of Barcelona (Spain) for their interest in this work, Dr. J.-G. Caputo from Institut National des Sciences Appliquées in Rouen for improving the English of the manuscript as well as K. Goździewski from Toruń University (Poland) for his computing and technical help. We thank O. Benois and G. Grancher from Department of Mathematics of University of Rouen and Dr. H. Ghidouche from De-

partment of Mathematics of University of Paris-Nord for their computer assistance during the preparation of the present paper.

The first, third and fourth authors want to thank their wives Prisque, Zbroja and Helena for their patience. The third and fourth authors thank also Rouen and Toruń Universities for their excellent working conditions during the authors' respective visits in August and in December 1992.

Last but not least, we thank the organizers of the Equadiff 91 conference where the observer method was presented for the first time.

Research of the third author was supported by KBN grant 22149203. During the final stage of work he was also supported by fellowship ERB3510-PL9210479 from the European Community's Action for Cooperation in Science and Technology with Central and Eastern European Countries.

References

- [1] M. Adler and P. van Moerbeke, *The algebraic integrability of geodesic flow on $SO(4)$* , Invent. Math. 67 (1982), 297–331.
- [2] V. I. Arnold, *Mathematical Methods of Classical Mechanics*, Graduate Texts in Math. 60, Springer, Berlin, 1989.
- [3] V. I. Arnold, V. V. Kozlov and A. I. Neishtadt, *Mathematical aspects of classical and celestial mechanics*, V. I. Arnold (ed.) *Dynamical Systems III*, Encyclopaedia Math. Sci. 3, Springer, Berlin, 1988.
- [4] M. Artigue, V. Gautheron et E. Isambert, *Ensemble de bifurcation et topologie des variétés intégrales dans le problème du solide pesant*, J. Méc. Théor. Appl. 5 (1986), 429–469.
- [5] M. Audin et R. Shilol, *Variétés abéliennes réelles et toupie de Kovalevski*, Publ. IRMA (preprint), Strasbourg, 1992.
- [6] J. Baumgarte, *Stabilization of the differential equations of Keplerian motion*, in: B. D. Tapley and V. Szebehely (eds.), *Recent Advances in Dynamical Astronomy*, Reidel, Dordrecht, 1973, 38–44.
- [7] —, *Stabilization, manipulation and analytic step adaptation*, in: V. Szebehely and B. D. Tapley (eds.), *Long Time Predictions in Dynamics*, Reidel, Dordrecht, 1976, 153–163.
- [8] G. Benettin, M. Casartelli, L. Galgani, A. Giorgilli and J.-M. Strelcyn, *On the reliability of numerical study of stochasticity. Part I: Existence of time averages*, Nuovo Cimento 44B (1978), 183–195.
- [9] —, —, —, —, *On the reliability of numerical study of stochasticity. Part II: Identification of time averages*, *ibid.* 50B (1979), 211–232.
- [10] D. G. Bettis (ed.), *Proceedings of the Conference on the Numerical Solution of Ordinary Differential Equations, 19–20 October 1972, the University of Texas at Austin*, Lecture Notes in Math. 362, Springer, Berlin, 1974.
- [11] O. I. Bogoyavlensky, *Integrable Euler equations on Lie algebras arising in problems of mathematical physics*, Math. USSR-Izv. 25 (1984), 207–257.
- [12] —, *Integrable Euler equations on $SO(4)$ and their physical applications*, Comm. Math. Phys. 93 (1984), 417–436.

- [13] O. I. Bogoyavlensky, *New integrable problems of classical mechanics*, *ibid.* 94 (1984), 225–269.
- [14] —, *Euler equations on finite dimensional Lie algebras arising in physical problems*, *ibid.* 95 (1984), 307–315.
- [15] —, *Periodic solutions in a model of pulsar rotation*, *ibid.* 102 (1985), 349–359.
- [16] —, *Integrable cases of a rigid body dynamics and integrable systems on the ellipsoids*, *ibid.* 103 (1986), 305–322.
- [17] —, *Some integrable cases of Euler equations I*, *Dokl. Akad. Nauk SSSR* 287 (1986), 1105–1108 (in Russian).
- [18] —, *Some integrable cases of Euler equations II*, *ibid.* 292 (1987), 318–322 (in Russian).
- [19] —, *Boundary value problems of mathematical physics*, *Proc. Steklov Inst. Math.* 95 (1988).
- [20] —, *Euler equations on finite dimensional Lie coalgebras*, *Uspekhi Mat. Nauk* 47 (1) (1992), 107–146 (in Russian); English transl.: *Russian Math. Surveys* 47 (1).
- [21] J. C. Butcher, *Implicit Runge–Kutta processes*, *Math. Comput.* 18 (1964), 50–64.
- [22] P. J. Channell and J. C. Scovel, *Symplectic integrators of Hamiltonian systems*, *Nonlinearity* 3 (1990), 231–259.
- [23] —, —, *Integrators for Lie–Poisson dynamical systems*, *Phys. D* 50 (1991), 80–88.
- [24] I. P. Cornfeld, S. V. Fomin and Ya. G. Sinai, *Ergodic Theory*, Springer, Berlin, 1982.
- [25] R. L. Devaney, *Homoclinic orbits in Hamiltonian systems*, *J. Differential Equations* 21 (1976), 431–438.
- [26] B. A. Dubrovin, A. T. Fomenko and S. P. Novikov, *Modern Geometry—Methods and Applications. Part I: The Geometry of Surfaces. Transformation Groups and Fields*, Graduate Texts in Math. 93, Springer, Berlin, 1984.
- [27] —, —, —, *Modern Geometry—Methods and Applications. Part II: The Geometry and Topology of Manifolds*, Graduate Texts in Math. 104, Springer, Berlin, 1985.
- [28] T. Eirola and J. M. Sanz-Serna, *Conservation of integrals and symplectic structure in the integration of differential equations by multistep methods*, *Numer. Math.* 61 (1992), 281–290.
- [29] El Hamidi, *Propriétés stochastiques d’un système non-linéaire en dimension finie*, Thèse de physique théorique, Université de Pau, 1989.
- [30] K. Feng and M.-Z. Qin, *The symplectic methods for the computation of hamiltonian equations*, in: Y.-W. Zhu and B.-Y. Guo (eds.), *Numerical Methods for Partial Differential Equations*, Lecture Notes in Math. 1297, Springer, Berlin, 1987, 1–37.
- [31] A. F. Filippov, *Differential Equations with Discontinuous Right Hand Side*, Nauka, Moscow, 1985 (in Russian).
- [32] A. T. Fomenko, *Integrability and Nonintegrability in Geometry and Mechanics*, Kluwer, Dordrecht, 1988.
- [33] A. T. Fomenko and V. V. Trofimov, *Integrable Systems on Lie Algebras and Symmetric Spaces*, Gordon and Breach, New York, 1988.
- [34] N. K. Gavrilov and L. P. Shil’nikov, *On bifurcations of the equilibrium states of a hamiltonian system with two degrees of freedom*, *Selecta Math. Sov.* 10 (1) (1991), 61–68.
- [35] Z. G. Ge and J. E. Marsden, *Lie–Poisson–Hamilton–Jacobi theory and Lie–Poisson integrators*, *Phys. Lett. A* 133 (3) (1988), 134–139.
- [36] C. W. Gear, *Invariants and numerical methods for ODEs*, *Phys. D* 60 (1992), 303–310.

- [37] B. Gladman and M. Dunca, *Symplectic integrators for long-term integrations in celestial mechanics*, *Celestial Mech.* 52 (1991), 221–240.
- [38] D. Greenspan, *Arithmetic Applied Mathematics*, Pergamon Press, Oxford, 1980.
- [39] J. W. Grizzle and P. E. Moraal, *Newton, observers and nonlinear discrete-time control*, in: Proc. 29th Conf. on Decision and Control, Honolulu, Hawaii, 1990, 760–767.
- [40] L. Haine, *Geodesic flow on $SO(4)$ and abelian surfaces*, *Math. Ann.* 263 (1983), 435–472.
- [41] —, *The algebraic complete integrability of geodesic flow on $SO(N)$* , *Comm. Math. Phys.* 94 (1984), 271–287.
- [42] E. Hairer, S. P. Norsett and G. Wanner, *Solving Ordinary Differential Equations I. Nonstiff Problems*, Springer, Berlin, 1987.
- [43] P. Hartman, *Ordinary Differential Equations*, Wiley, New York, 1964.
- [44] K. Hockett, *Chaotic numerics from an integrable hamiltonian system*, *Proc. Amer. Math. Soc.* 108 (1990), 271–281.
- [45] V. D. Irtegov, *Invariant Manifolds of Stationary Motions and Their Stability*, Nauka, Siberian branch, Novosibirsk, 1985 (in Russian).
- [46] H. Kinoshita, H. Yoshida and H. Nakai, *Symplectic integrators and their application to dynamical astronomy*, *Celestial Mech.* 50 (1991), 59–71.
- [47] A. M. Kovalev and A. N. Chudnenko, *On stability of the equilibrium point of a Hamiltonian system with two degrees of freedom in the case of equal frequencies*, *Dokl. Akad. Nauk Ukrain. SSSR Ser. A* 11 (1977), 1010–1013 (in Russian).
- [48] V. V. Kozlov, *Integrability and nonintegrability in hamiltonian mechanics*, *Uspekhi Mat. Nauk* 38 (1) (1983), 3–67 (in Russian).
- [49] V. V. Kozlov and D. A. Onishenko, *Nonintegrability of Kirchhoff equations*, *Dokl. Akad. Nauk SSSR* 266 (1982), 271–281 (in Russian).
- [50] J. D. Lambert, *Computational Methods in Ordinary Differential Equations*, Wiley, New York, 1973.
- [51] M. Lecar, *A comparison of eleven numerical integrations of the same gravitational 25-body problem*, *Bull. Astronom. Sér.* 3 vol. III fasc. 1 (1968), 91–104.
- [52] E. Leimanis, *The General Problem of the Motion of Coupled Rigid Bodies about a Fixed Point*, Springer, Berlin, 1965.
- [53] L. M. Lerman and Ya. L. Umanskiĭ, *On the existence of separatrix loops in four-dimensional systems similar to the integrable hamiltonian systems*, *J. Appl. Math. Mech.* 47 (3) (1983), 335–340.
- [54] T. Levi-Civita and G. Amaldi, *Lezioni di meccanica razionale*, Vol. II, Part 2, Zanichelli, Bologna, 1927.
- [55] A. J. Lichtenberg and M. A. Lieberman, *Regular and Stochastic Motion*, *Appl. Math. Sci.* 38, Springer, Berlin, 1983.
- [56] A. J. Maciejewski and J.-M. Strelcyn, *Numerical integration of differential equations in presence of first integrals: partial first integrals*, to appear.
- [57] A. Marciniak, *Numerical Solutions of the n-Body Problem*, Reidel, Dordrecht, 1985.
- [58] —, *The Selected Numerical Methods for Solving the n-Body Problem*, Poznań Technical University, 1989.
- [59] A. Marciniak and D. Greenspan, *Energy conserving numerical solutions of simplified turbulence equations*, Dept. Math., the University of Texas at Arlington, Technical Report 269, 1990.
- [60] —, —, *Arbitrary order Hamiltonian conserving numerical solutions of Calogero and Toda systems*, *Computers Math. Appl.* 22 (7) (1991), 11–35.

- [61] P. E. Nacozy, *The use of integrals in numerical integrations of the n-body problem*, *Astrophys. and Space Sci.* 14 (1971), 40–51.
- [62] O. Neron de Surgy, *Sur les intégrateurs symplectiques pour les systèmes Hamiltoniens standards et les systèmes de Lie–Poisson; une application aux équations d’Euler sur $SO(4)$* , Rapport de stage fait à Electricité de France, 1991.
- [63] P. J. Olver, *Applications of Lie Groups to Differential Equations*, Graduate Texts in Math. 107, Springer, Berlin, 1986.
- [64] S. A. Orszag and J. B. McLaughlin, *Evidence that random behavior is generic for nonlinear differential equations*, *Phys. D* 1 (1980), 68–79.
- [65] A. M. Perelomov, *Dynamical systems of classical mechanics with hidden symmetry*, Preprints Inst. Theor. Exper. Phys. Moscow 82, 1981 (in Russian).
- [66] —, *Integrable systems of classical mechanics and Lie algebras. The simplest systems*, Preprints Inst. Theor. Exper. Phys. Moscow 149, 1981 (in Russian).
- [67] —, *Integrable systems of classical mechanics and Lie algebras. Constrained systems*, Preprints Inst. Theor. Exper. Phys. Moscow 116, 1983 (in Russian).
- [68] —, *Integrable systems of classical mechanics and Lie algebras. The motion of a rigid body with fixed point*, Preprints Inst. Theor. Exper. Phys. Moscow 147, 1983 (in Russian).
- [69] —, *Integrable systems of classical mechanics and Lie algebras. The motion of a rigid body in the ideal fluid*, Preprints Inst. Theor. Exper. Phys. Moscow 151, 1984 (in Russian).
- [70] —, *Integrable Systems of Classical Mechanics and Lie Algebras*, Vol. I, Birkhäuser, Basel, 1990.
- [71] H. Pollard, *Celestial Mechanics*, Carus Math. Monogr. 18, Math. Assoc. Amer., 1976.
- [72] J. M. Sanz-Serna, *Symplectic integrators for Hamiltonian problems: an overview*, *Acta Numerica* 1992, 243–286.
- [73] Ya. G. Sinai *et al.*, *Ergodic theory with applications to dynamical systems and statistical mechanics*, in: Ya. G. Sinai (ed.), *Dynamical Systems II*, Encyclopaedia Math. Sci. 2, Springer, Berlin, 1989.
- [74] S. Smale, *Topology and mechanics. I*, *Invent. Math.* 10 (1970), 305–331.
- [75] —, *Topology and mechanics. II*, *ibid.* 11 (1970), 45–64.
- [76] A. G. Sokol’skiĭ, *On the stability of an autonomous hamiltonian system with two degrees of freedom in the case of equal frequencies*, *J. Appl. Math. Mech.* 38 (1974), 741–749.
- [77] E. Stiefel and G. Schiefefe, *Linear and Regular Celestial Mechanics*, Springer, Berlin, 1971.
- [78] J.-M. Strelcyn, *The “coexistence problem” for conservative dynamical systems: a review*, *Colloq. Math.* 62 (1991), 331–345.
- [79] V. V. Strygin and V. A. Sobolev, *Separation of Motions by the Method of Integral Manifolds*, Nauka, Moscow, 1988 (in Russian).
- [80] V. V. Trofimov, *Introduction to the Geometry of Manifolds with Symmetries*, Moscow University Press, Moscow, 1989.
- [81] S. Ushiki, *Central difference schema and chaos*, *Phys. D* 4 (1982), 407–424.
- [82] A. P. Veselov, *On conditions of integrability of Euler equations on $SO(4)$* , *Dokl. Akad. Nauk SSSR* 270 (1983), 1298–1300 (in Russian).
- [83] H. Yoshida, *Construction of higher order symplectic integrators*, *Phys. Lett. A* 150 (1990), 262–268.

ERIC BUSVELLE
CENTRE DE RECHERCHE SHELL S.A.
BOÎTE POSTALE 20
76530 GRAND-COURONNE, FRANCE

RACHID KHARAB
DÉPARTEMENT DE MATHÉMATIQUES
UNIVERSITÉ DE ROUEN
URA CNRS 1378
76821 MONT SAINT AIGNAN, FRANCE
E-mail: KHARAB@UNIV-ROUEN.FR

JEAN-MARIE STRELCYN
DÉPARTEMENT DE MATHÉMATIQUES
UNIVERSITÉ DE ROUEN
URA CNRS 1378
76821 MONT SAINT AIGNAN, FRANCE
E-mail: STRELCYN@UNIV-ROUEN.FR

A. J. MACIEJEWSKI
INSTITUTE OF ASTRONOMY
NICHOLAS COPERNICUS UNIVERSITY
UL. CHOPINA 12/18
87-100 TORUŃ, POLAND
E-mail: MACIEJKA@ASTRI.UNI.TORUN.PL

and

LABORATOIRE ANALYSE, GÉOMÉTRIE
ET APPLICATIONS, URA 742
DÉPARTEMENT DE MATHÉMATIQUES
UNIVERSITÉ PARIS-NORD, INSTITUT GALILÉE
AVENUE J.-B. CLÉMENT
93430 VILLETANEUSE, FRANCE
E-mail: STRELCYN@MATH.UNIV-PARIS13.FR

Received on 15.12.1993